令和 2 年度　博士論文

Gas-phase preparation and characterization of photocatalytic Ag-TiO_2 nanoparticulate thin films

（Ag-TiO_2 光触媒ナノ粒子薄膜の気相作製と特性評価）

指導教員：島田　学　教授

Supervisor: Professor Manabu Shimada

広島大学大学院工学研究科　化学工学専攻

Graduate School of Engineering Hiroshima University

Department of Chemical Engineering

キョウ　デンペイ

姜　殿平

2021 年 3 月

Abstract

Titanium dioxide (TiO_2), as a promising photocatalyst, has been the object of extensive investigation in recent years because of its excellent property in air and water purification. The loading of Ag nanoparticles on the TiO_2 supporting materials is considered as an effective method to enhance the photocatalytic property of TiO_2 by inhibiting the recombination of electron-hole pairs and broadening the light absorbance spectrum from UV region to visible region.

In this dissertation, the photocatalytic Ag-TiO_2 nanoparticulate thin films were fabricated via a combined plasma-enhanced chemical vapor deposition (PECVD) system and physical vapor deposition (PVD) system. The properties and performance of the prepared photocatalytic materials were studied. The major contents of this thesis are listed as follows.

In **chapter 1**, the background, review of previous researches, motivation and goal of this research were introduced.

In **chapter 2**, Ag-TiO_2 nanoparticulate thin films were fabricated via a combined PECVD and PVD processes. The films were fabricated on a silicon substrate by the simultaneous deposition of TiO_2 and Ag nanoparticles synthesized by the new process. Then the effects of the Ag nanoparticles on the photocatalytic activity of fabricated nanoparticulate films were studied. The results indicated that the loading of Ag nanoparticles influenced the morphology and crystal structure of the TiO_2 nanoparticles in the Ag-TiO_2 nanoparticulate films. The photocatalytic performance of the fabricated

Ag-TiO_2 nanoparticulate films evaluated from the rate of degradation of methylene blue under UV light irradiation was found to be 35% greater than a film consisting of pristine TiO_2.

In **chapter 3**, the effects of heat treatment of the Ag-TiO_2 nanoparticulate films on the morphology, crystal structure, and photocatalytic activity were investigated. The thin films prepared by following the processes developed in the previous chapter were annealed at different temperatures. The changes of annealing temperature were found evidently influence the particle size, crystal structure, crystallite size, phase content, and photocatalytic activity of fabricated Ag-TiO_2 nanoparticulate films. The optimal photocatalytic activity of fabricated Ag-TiO_2 nanoparticulate films was obtained at an annealing temperature of 700 °C. The phase content of the fabricated Ag-TiO_2 nanoparticulate films was 77% anatase phase and 23% rutile phase. The relationship between the photocatalytic activity and the phase content in the Ag-TiO_2 nanoparticulate films was evaluated and the result indicated that the photocatalytic activity decreases in the order of mixture of anatase-rutile > pure anatase > pure rutile.

In **chapter 4**, the effects of Ag concentration in the Ag-TiO_2 nanoparticulate films on the morphology, crystal structure, light absorption capability, and photocatalytic activity were investigated. The Ag concentration in the Ag-TiO_2 nanoparticulate films changed by tuning the conditions for the PVD process to generate Ag nanoparticles in different amount. The Ag nanoparticles were well dispersed and tightly attached on the surface of TiO_2 nanoparticles in the film. The morphology, particle size, light absorbance

and photocatalytic activity of Ag-TiO_2 nanoparticulate films were evidently affected by the Ag content. Evaluation of the photocatalytic activity under UV light irradiation showed that an Ag concentration of 2.2 wt% yielded the optimal photocatalytic performance, which was 5.5 times higher than that of the TiO_2 film. The photocatalytic activity was also measured under visible light irradiation. The optimal photocatalytic activity of the Ag-TiO_2 films in visible light was 2.4 times better than that of the TiO_2 film when the Ag concentration was 0.24 wt%.

Chapter 5 highlights the summary of each chapter. Suggestions for further research on Ag-TiO_2 photocatalytic films are also proposed.

Contents

Chapter 1

Introduction

1.1 Background

With the rapid growth of human activities, it becomes crucial to reduce the combustion of fossil fuels and industrial pollutions which have negative effects on the continued development of human society. Developing efficient photocatalyst is considered as a promising way to minimize the environmental pressure and utilize renewable solar energy. Based on the photocatalysis, a wide range of applications such as water purification (Lee and Park, 2013), air purification (Paz, 2010), solar cells (Hirakawa and Kamat, 2005； Han *et al.*, 2012), disinfection (Hirakawa and Kamat, 2005) and water splitting (Fujishima and Honda, 1972) have been developed.

In recent decades, titanium dioxide (TiO_2) has drawn great attention in the field of photocatalysis due to its suitable band gap, strong oxidation capacity, low cost, good chemical and physical stability, and high refractive index (Fujishima *et al.*, 2008； Paz, 2010； Tan *et al.*, 2011； Schneider *et al.*, 2014). Moreover, various methods have been approached to improve the photocatalytic activity of TiO_2. For example, surface modification on TiO_2, especially noble metal loading, can broaden the light absorbance in visible light field and increase the photocatalytic performance. Many researchers have reported that the addition of Ag can improve the photocatalytic activity of TiO_2 (Sung-Suh *et al.*, 2004； Yu *et al.*, 2005； Chen *et al.*, 2013).

In addition, the TiO_2 nanoparticles and modified TiO_2 nanocomposites without aggregation and agglomeration exhibit large surface area which is beneficial to the photocatalytic performance. Therefore, the efficient preparation method of TiO_2 nanoparticles and modified TiO_2 nanocomposites in small scale is also a task for the practical applications.

In this introduction, structural characteristics of TiO_2, surface modification on TiO_2 and fabrication methods for TiO_2 nanoparticles and Ag-TiO_2 nanocomposites will be described briefly.

1.2 Ag-TiO_2 heterogeneous photocatalyst

1.2.1 Applications of TiO_2

In recent decades, the research on the TiO_2 is a field of continuous expansion. TiO_2 has been used for many applications in different fields such as pigments, food additives, self-cleaning surfaces, ultraviolet protection cosmetics, solar cells and biocides due to its strong oxidation capacity, suitable band gap, low cost, good chemical and physical stability, and high refractive index (Hirakawa and Kamat, 2005； Schneider *et al.*, 2014). Among various applications, the photocatalysis of TiO_2 draws the most attention. In 1970s, the photocatalysis for water splitting was achieved by using a single crystal n-type TiO_2 electrode. After their pioneering work, semiconductor photocatalyst (especially TiO_2) has attracted a great deal of attention in the aspects of energy and environment. Fig. 1.1 shows various applications of TiO_2 photocatalysis (Hussein and Shaheed, 2015).

Based on the photocatalysis of TiO_2, a wide range of useful applications such as solar cells, sensors, water and air purification, disinfection and hydrogen evolution have been developed.

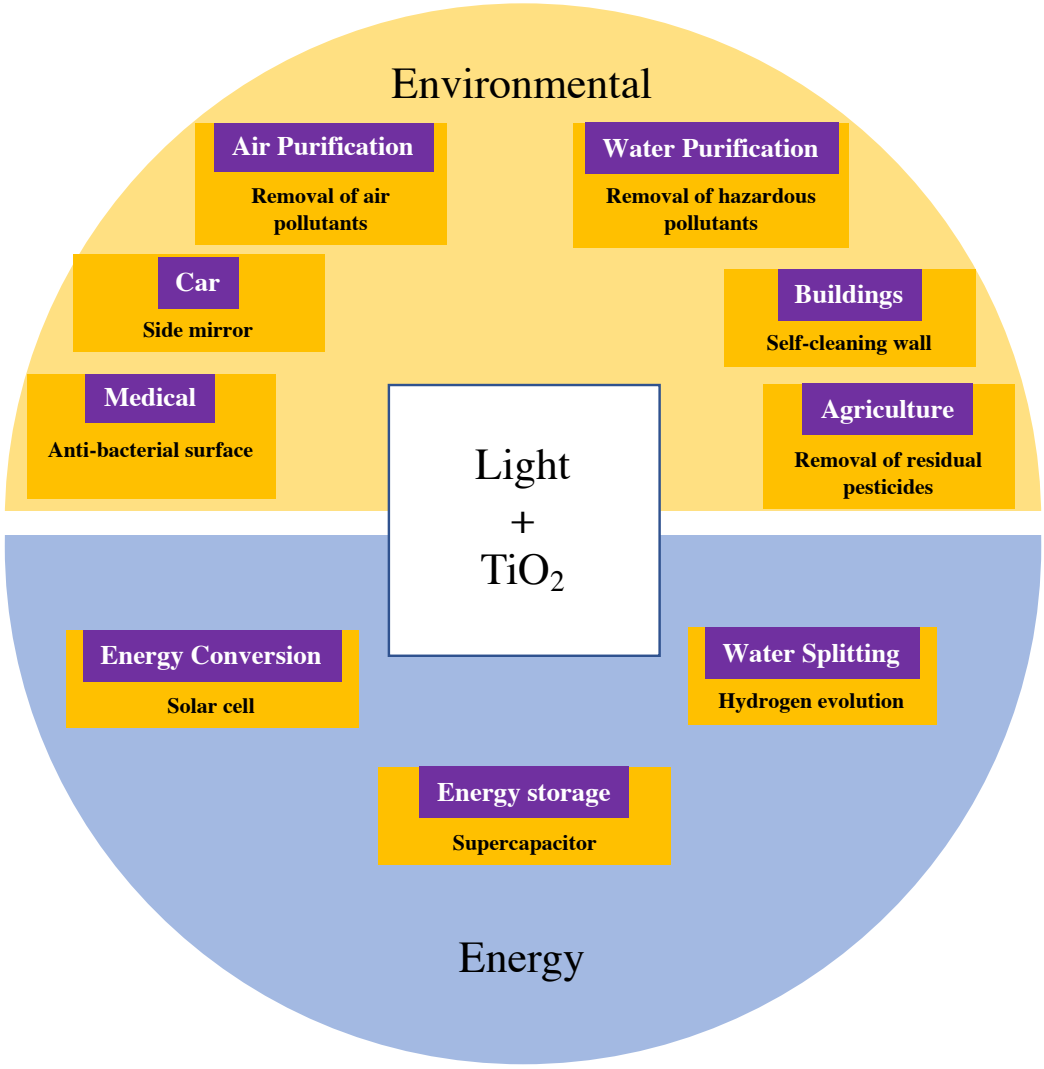

Fig. 1.1 Applications of TiO_2 photocatalysis in environmental and energy aspects.

1.2.2 The photocatalysis of TiO_2

The photocatalytic properties of TiO_2 are derived from its unique the band gap as a semiconductor. Fig. 1.2 shows the schematic illustration of the generation of

photogenerated electrons and holes in TiO_2 under UV light irradiation and the following photocatalytic reaction. When TiO_2 is irradiated by UV from solar power or artificial light, the photoelectrons in the valence band are excited and jump to the conduction band of TiO_2 which result in creating the photogenerated electron and hole pairs in the TiO_2 structure. This is the photo-excitation state in semiconductor (Schneider *et al.*, 2014).

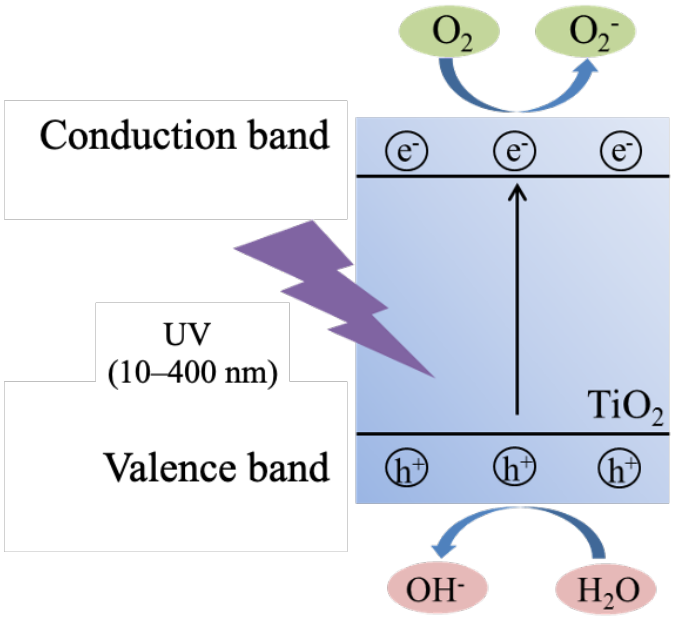

$$TiO_2 + h\nu \leftrightarrow h^+ + e^-$$

$$h^+ + H_2O_{absorbed} \leftrightarrow H^+ + {}^{\bullet}OH$$

$$e^- + O_{2\ absorbed} \leftrightarrow {}^{\bullet}O_2^-$$

Fig. 1.2 Schematic illustration of the generation of photogenerated electrons and holes in TiO_2 irradiated by UV light and the following photocatalytic reaction.

The photogenerated holes in the valence band and electrons in the conduction band will transfer to the surface of TiO_2 and participated in the photocatalytic reaction with surrounding materials like water, oxygen. The hydroxyl radicals (radical ·OH) will generate after the oxidation reaction between photogenerated holes and absorbed water. While electrons in the conduction band will react with absorbed oxygen to produce superoxide radical anions ($O_2^{\cdot-}$). The produced superoxide radical anions ($O_2^{\cdot-}$) gets protonated forming hydroperoxyl radical ($HO_2^{\cdot}$) and then subsequently H_2O_2. In the last, the generated H_2O_2 dissociates into hydroxyl radicals (·OH). Due to the powerful ability to oxide organic molecules, the generated hydroxyl radicals (·OH) play a key role for the oxidative destruction of organic molecules in photocatalytic reactions.

1.2.3 Crystal structures of TiO_2

There are three kinds of naturally occurring oxides of TiO_2 at atmospheric pressure named by anatase, brookite, and rutile. The different 3D arrangements of the TiO_2 phases was reported by the previous study (Pal and Pal, 2015). The structural variation in the different polymorphs is ascribe to the different ways in sharing of edges and corners between adjacent TiO_6 octahedral units. Each cubic space contains several TiO_6 octahedral units. The anatase phase is built by sharing edges of adjacent TiO_6 octahedral units, while the rutile and brookite frameworks consisted of the mixed corner- and edge-sharing configurations in various ways (Pal and Pal, 2015).

These polymorphs exhibit various stability and property and various photocatalytic performances. Rutile is the stable phase but the phase of anatase and brookite show less stability than rutile. The metastable anatase transforms irreversibly to rutile at elevated temperatures. The band gap of rutile 3 eV while that of anatase is 3.2 eV. It is also reported that the anatase phase shows better photocatalytic activity than the rutile phase (Luttrell *et al.*, 2014).

The differences in the stability and property of different phases in TiO_2 origins form the different lattice structures in symmetry, coordination number, and Ti-Ti bond distance (Tang *et al.*, 1993). The symmetry in anatase is worse than that of rutile because the octahedron is significantly distorted. The coordination number of single TiO_6 octahedral unit in anatase (4 sharing one edge, 4 sharing one corner) is smaller than that of in rutile (2 sharing one edge, 8 sharing one corner). Hence, the rutile phase is denser and more stable than the anatase phase. Moreover, the symmetry of the Ti influences band splitting which results in varying degrees in electronic band structures.

1.2.4 Surface modification of TiO_2 by noble metal nanoparticles

It has been widely reported that surface modification of TiO_2 with metal nanoparticles could improve its photocatalytic activity, especially with the noble metals such as Pt, Au, Cu, Ag, and Pd (Sun *et al.*, 2003； Linic *et al.*, 2011). The mechanism of enhanced photocatalytic activity of Ag-TiO_2 nanocomposite is shown in Fig. 1.3. Due to the work function of noble metal is greater than that of the semiconductor such as TiO_2, a Schottky barrier is created when the noble metal contract with the semiconductor. The metallic nanoparticles act as the electron trap which trap the photogenerated electrons from TiO_2 and create separated electron-hole pairs. The separated electron-hole pairs can react with water and oxygen to generate more •OH and $\bullet O_2^-$ on the surface of TiO_2 in resulting higher photocatalytic activity.

TiO_2, as a semiconductor, has a band gap of 3.2 eV for anatase, 3.0 eV for rutile. Due to the characteristic band gap, the photoelectron can be produced in TiO_2 under UV light irradiation (under 400 nm). However, the photogenerated electrons can be produced in Ag under visible irradiation due to the localized surface plasmon resonance (LSPR) phenomenon(Sellappan *et al.*, 2013). The addition of Ag nanoparticles can broaden the light absorbance spectrum of TiO_2 and make Ag-TiO_2 nanocomposite photocatalyst is available in either UV region or visible region.

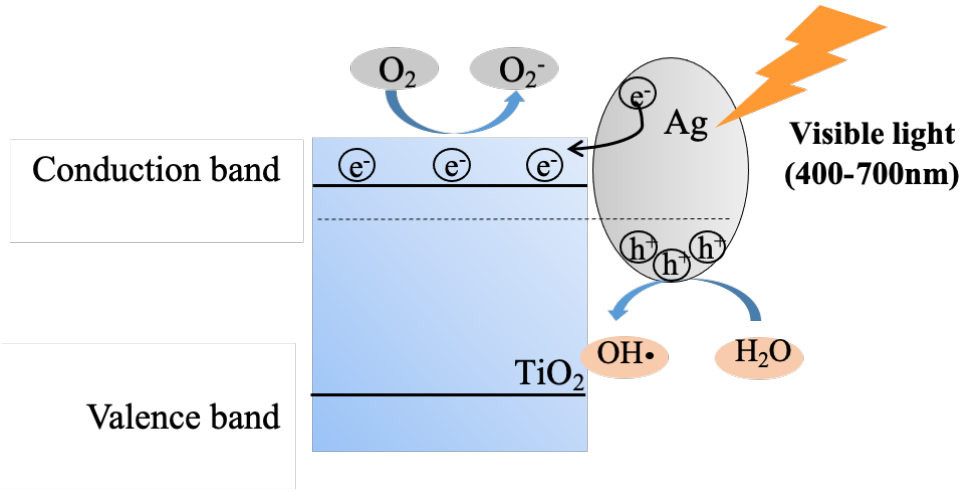

Fig. 1.3 The mechanism of enhanced electron-hole separation caused by addition Ag nanoparticle on the TiO_2 surface.

1.3 Preparation methods for Ag and TiO_2 nanoparticles

1.3.1 Preparation methods for nanoparticles

Nanoparticles have drawn great attention due to its unique properties in optical, electronic, magnetic and catalytic fields. Varieties of synthesis methods for nanoparticles have been used which can be classified as solid-phase method, liquid-phase method and gas-phase method.

1.3.1.1 Solid-phase method

The solid-phase method for preparing nanoparticles is to mill the source materials into nanoparticles for a long time. The impurity coming from the milling tools is easy to contaminate the prepared materials. The narrowed size distribution in prepared nanoparticles is hard to obtain (Gupta and Kant, 2013). Particle size of prepared

nanoparticles is related to a series of factors such as milling time, milling collision energy, milling temperature, and so on (Ghorbani, 2014).

1.3.1.2 Liquid-phase method

The liquid-phase methods are the most popular method in nanoparticle synthesis involving chemical precipitation process. The particle size or shapes of prepared nanoparticles can be controlled in nucleation and particle growth stages. The liquid-phase methods have the advantages of fabricating nanoparticles in complex shapes and controllable particle size. However, there are some disadvantages such as involving complex fabrication steps, long preparation time and residues removal process.

1.3.1.3 Gas-phase method

Fig. 1.4 shows the detailed schematic process of preparation of nanoparticles and nanoclusters by gas-phase method (Gupta and Kant, 2013). The gas-phase method involves chemical reactions to generate condensable gaseous species. The activation energy of chemical reactions (usually decomposition reactions) is mostly supplied by high temperature in flame, laser and plasma filed. The nanoparticles can be produced by the condensation of supersaturated vapor. Generally, the gas-phase methods show advantages such as convenience for preparation and reduced opportunities for contamination and uniform morphological structure of the product.

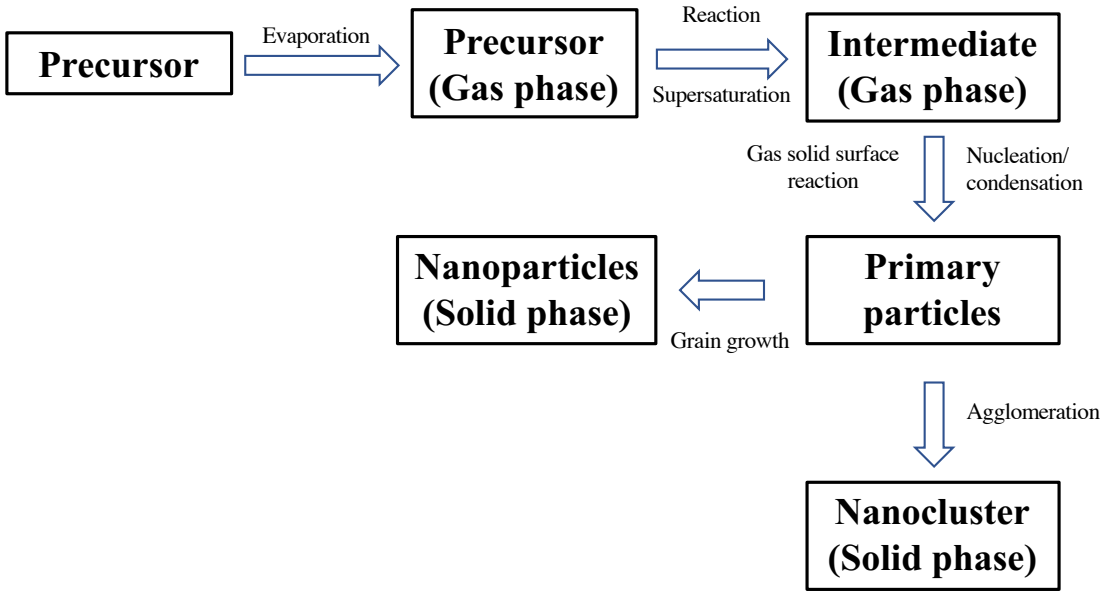

Fig. 1.4 Schematic process for the preparation of nanoparticles and nanocluster by gas-phase method (Gupta and Kant, 2013).

1.3.2 Liquid-phase methods for preparing Ag or TiO_2 nanoparticles

1.3.2.1 Chemical reduction of Ag ions

The most used method for preparation of Ag nanoparticles is chemical reduction by organic and inorganic reducing agents. Various reducing agents (Lee *et al.*, 2005； Geetha *et al.*, 2015； Avciata *et al.*, 2016； Chowdhury *et al.*, 2016) such as sodium citrate, ascorbate, Tollens reagent, sodium, polyol process, borohydride ($NaBH_4$), L-tyrosine, polyols, ascorbic acid, polyethylene glycol and N, N-dimethylformamide (DMF) are used for the reduction of Ag ions (Ag^+) in aqueous solutions. The metallic silver (Ag^0) nanoparticles can be formed by the reduction reaction between reducing agents and Ag^+ (Iravani *et al.*, 2014).

1.3.2.2 Sol-gel method

The sol-gel method is a popular approach in preparing different materials especially for SiO_2 and TiO_2 nanoparticles. A colloidal suspension (sol) can be produced by the hydrolysis and polymerization reactions of the precursors. The liquid sol will turn into a solid gel and then becomes a dense ceramic after a series of processes of polymerization, loss of solvent, drying and heat treatment. Thin films can also be prepared by spin-coating or dip-coating methods with combination of the sol-gel method. (Malekshahi Byranvand *et al.*, 2013). The sol-gel method has advantages such as versatility of processing in atmosphere conditions and homogeneity but the disadvantages like involving impurities and complex steps cannot be ignored.

1.3.2.3 Hydrothermal Method

Hydrothermal method involves aqueous solutions in an autoclave with controlling of temperature or pressure. The crystalized materials be produced from high-temperature aqueous solutions at high vapor pressures. The internal pressure of the autoclaves can be influenced by the temperature and the amount of solution (Malekshahi Byranvand *et al.*, 2013). Hydrothermal method has advantages in obtaining crystalized material at appropriate crystallization temperature, controllable reaction conditions, low energy cost. Gomathi Thanga Keerthana *et al*. reported the TiO_2 nanotubes (24 nm) and nanorods (30 nm) were successfully prepared by using different solvents (Gomathi Thanga Keerthana *et al.*, 2018).

1.3.2.4 Photodeposition Method

The photodeposition method (Nishizawa, 1988) is a popular way to prepare metal-semiconductor nanocomposites. When semiconductor materials are irradiated by proper energy which is larger than the band gap, the photoelectrons will be excited. The photo electrons will transfer to the metal ion when the reduction potential of the metal ion is more positive than the conduction band energy level of the semiconductor. Then the metal ions can be reduced to metallic nanoparticles on the surface of semiconductor materials. The semiconductor with large surface area is considered as a good template for metal deposition. The photodeposition method is a simpler method to introduce metal nanoparticles in comparing with the methods involving chemical reagents, but the template materials with large surface area are still needed prepared.

1.3.3 Gas-phase methods for preparing Ag or TiO_2 nanoparticles

1.3.3.1 Spray pyrolysis

In the spray pyrolysis, a droplet containing a solute is evaporated or dissociated by a chemical reaction. A supersaturated solution in the droplet will be produced in the process of shrinkage following with the nucleation and particle growth stages. The schematic of flame spray pyrolysis for metal oxides is shown in Fig. 1.5. Spray pyrolysis normally results in hollow-shape particles in micron size. The spray pyrolysis process can be considered as a combined gas-phase method and liquid-phase method, because the

droplets are transported as aerosol but the particle generation in the droplets is a liquid phase process (Kruis *et al.*, 1998).

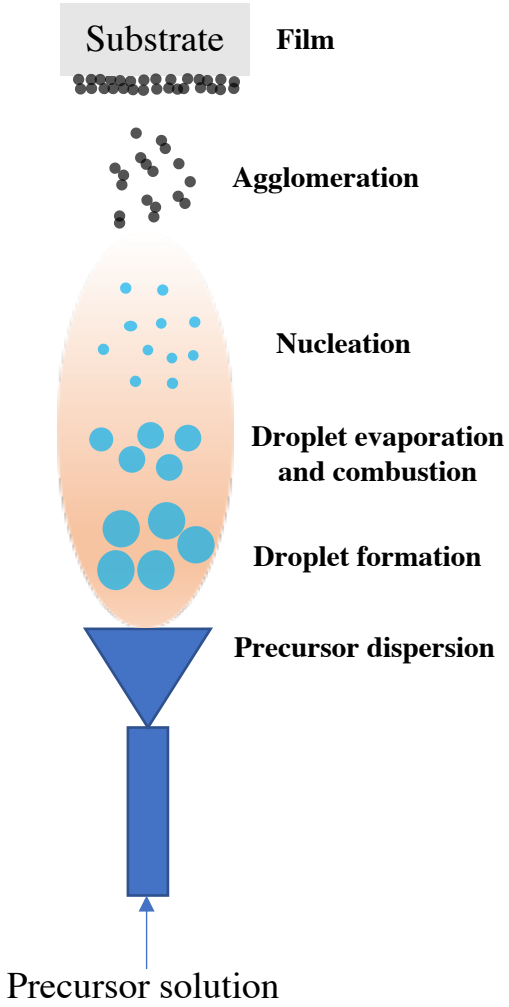

Fig. 1.5 The schematic of flame spray pyrolysis for materials.

1.3.3.2 Sputtering

Sputtering is the thin film deposition technique on an atomic level by vaporizing materials from a solid surface by bombardment with high-velocity ions of an inert gas (Ar or Kr), causing an ejection of atoms and clusters (Kruis *et al.*, 1998). The schematic of sputtering method for metal oxides is shown in Fig. 1.6.

Sangpour *et al*. fabricated TiO_2 films with Ag by using RF reactive magnetron cosputtering technique. The Ag atom and Ti atoms were sputted on the substrate with the mixture of argon and oxygen (Sangpour *et al.*, 2010).

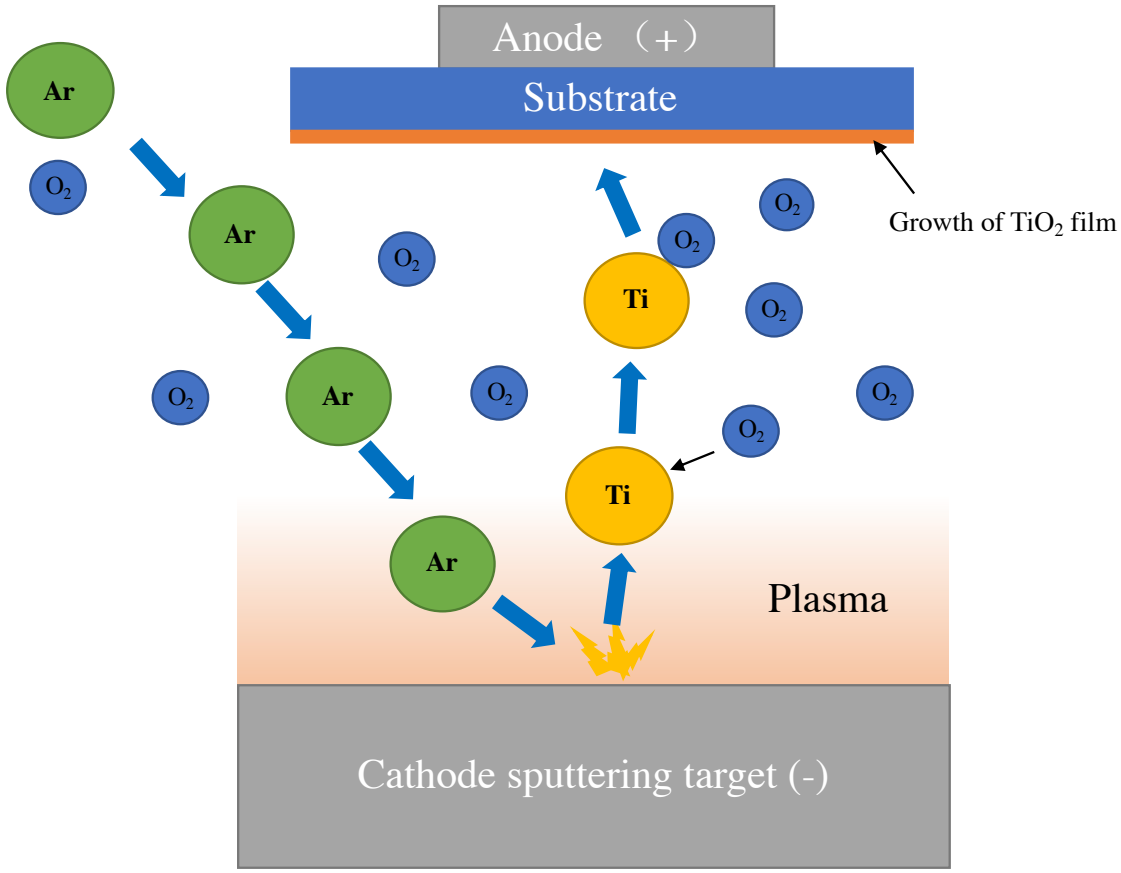

Fig. 1.6 The schematic of sputtering method for metal oxides (Sangpour *et al.*, 2010).

1.3.3.3 Physical vapor deposition (PVD)

Evaporation-condensation is one of the most important physical approaches to fabricate nanoparticles. The solid material put into a crucible can be vaporized at a high environment in the furnace. Nanoparticles can be produced by a natural cooling or

dilution cooling system. Nanoparticles in small size can be easily prepared by a rapid temperature decrease (Kruis *et al.*, 1998). Harra *et al*. (Harra *et al.*, 2012) prepared Ag nanoparticles with the PVD technique and evaluated the effect of heating temperature on the size distribution of generated Ag nanoparticles. The average particle size increases with increasing heating temperature.

1.3.3.4 Chemical vapor deposition (CVD)

A typical CVD process is consisted of a gas supply system, a deposition chamber and an exhaust system. In the deposition chamber, volatile precursors turn into nanoparticles after oxidation reactions or decomposition reactions and then deposit on a substrate. Usually, the activation energy for the chemical reaction is high temperature.

Pazoki *et al*. reported the preparation of TiO_2 nanoparticles using CVD technique (Pazoki *et al.*, 2012). The CVD setup has different sample zone. The different sample zone can prepare the TiO_2 material in different shapes.

1.3.3.5 Plasma enhanced chemical vapor deposition (PECVD)

The PECVD process is similar like the CVD process, but activation energy is from the plasma field. The PECVD method has advantages in fabricating materials in low temperature, low agglomeration, narrow size distributions and uniform thickness.

Kubo *et al*. reported the fabrication of non-agglomerated TiO_2 nanoparticles and SiO_2 using PECVD technique (Fig. 1.7). The residence time of nanoparticles and

precursor content were evaluated to obtain the non-agglomerated TiO_2 nanoparticles with narrow size distributions. The TiO_2 films with highly uniform pore structures were fabricated by electrostatic deposition.

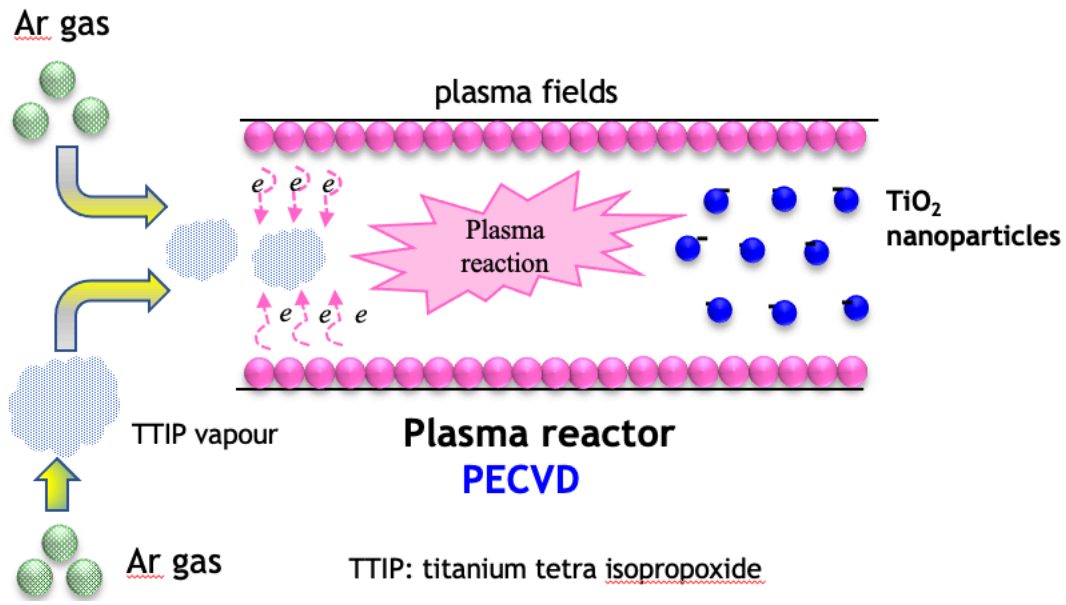

Fig. 1.7 The setup of PECVD technique for the preparation of non-agglomerated TiO_2 nanoparticles (Kubo *et al.*, 2013).

1.4 Reviews of materials reported in the dissertation

1.4.1 Preparation methods of Ag-TiO_2 heterogeneous photocatalyst

Ag-TiO_2 heterogenous photocatalyst is famous for its excellent photocatalytic activity both in UV region and visible region. Preparation of Ag-TiO_2 heterogeneous photocatalyst can be classified as liquid-phase method and gas-phase method.

Ag-TiO_2 nanocomposite powders were prepared by a sol-gel method which is considered as a liquid-phase method. Titanium isopropoxide (TTIP), $AgNO_3$, and N, N-dimethylformamide (DMF) were introduced to preparing Ag-TiO_2 nanocomposite powders after a series of preparations steps such as stirring, aging, washing, and annealing (Zhang and Chen, 2009). DMF is used as a reducing agent to prepare small Ag nanoparticles (3, 15 nm) by reducing $AgNO_3$. Ag-TiO_2 film also prepared by the method of spin coating (Halin *et al.*, 2018) after a sol-gel method using titanium isopropoxide (TTIP) and $AgNO_3$. Zhao *et al*. reported the preparation of Ag-TiO_2 heterogeneous photocatalyst can prepared the combination of sol-gel method and dip-coating method(Zhao and Chen, 2011).

Ma *et al*. reported the photo-deposition method to prepare Ag-TiO_2 composite spheres. The anatase TiO_2 spheres were originated from Tetrabutyl titanate ($Ti(OBu)_4$) via 450 °C annealing. The Ag nanoparticles were deposited on the surface of TiO_2 spheres under irradiation of a high-pressure mercury lamp (Ma *et al.*, 2014).

A hydrothermal method was applied to fabricate Ag-TiO_2 nanocomposite. The start materials ($AgNO_3$ and TTIP) and various reducing agents (ascorbic acid, sodium dodecyl

sulphate, $NaBH_4$, Hydrazine, PEG-600) were mixed and put into a high pressure and high temperature reactor (180 °C, 2h) for the hydrothermal synthesis. Ag-TiO_2 nanotubes were also prepared by Zhang *et al*. with the hydrothermal method (Zhang *et al.*, 2017).

On the other hand, the gas-phase methods were also used to prepare Ag-TiO_2 heterogeneous photocatalyst. Zhao *et al*. have used an ultrasonic spray pyrolysis method to fabricate Ag-TiO_2 nanocomposites. nanoparticles. The droplets containing spraying solution ($AgNO_3$ and P25) generated by ultrasonic nebulizer passed through a diffusion dryer and a heating zone sequentially. Then the Ag nanoparticles were formed by the thermal decomposition of $AgNO_3$ and deposited on the surface of TiO_2 nanoparticles (Zhao *et al.*, 2012). Flame spray pyrolysis was also applied to fabricate Ag-TiO_2 nanocomposites. TTIP and silver benzoate were dissolved in acetonitrile/xylene mixture and transported to a burner by oxygen flow. The Ag-TiO_2 powder consisted of Ag_2O were generated after combustion and collected by a filter (Gunawan *et al.*, 2009). Sanzone *et al*. reported Ag-TiO_2 nanocomposite layer was prepared by sputtering method involving Ti layer deposition, Ag layer deposition and annealing processes. Ag nanoparticles were prepared via thermal dewetting at 400 °C (Sanzone *et al.*, 2018).

The preparation methods of Ag-TiO_2 nanocomposites and features are shown in Table. 1.1. The most popular methods for Ag-TiO_2 nanocomposite are liquid-phase methods such as sol-gel method, photodeposition method and hydrothermal method. However, these methods have disadvantages such as involving complex fabrication steps, long preparation time and residues removal process. Generally, the gas-phase methods

show advantages such as convenience for preparation and reduced opportunities for contamination and uniform morphological structure of the product. But in ultrasonic spray pyrolysis (Zhao *et al.*, 2012) and flame spray pyrolysis (Gunawan *et al.*, 2009), the agglomeration of nanoparticles is easy to form in the high temperature environment for pyrolysis reaction and deposition. Sputtering method is difficult to control the structure in molecule level. Therefore, a simple controllable solventless gas-phase process without particle agglomeration is promising for the preparation of Ag-TiO_2 nanoparticles.

Table 1.1 Preparation methods of Ag-TiO_2 nanocomposites and features.

Methods	**Starting materials**	**Preparation of Ag nanoparticles**	**References**
Sol-gel	TTIP and $AgNO_3$	$AgNO_3$ were reduced by DMF	Zhang and Chen, 2009
Sol-gel and spin coating	TTIP and $AgNO_3$	Thermal decomposition of $AgNO_3$ annealed at 450 °C	Halin *et al*., 2018
Sol-gel and dip-coating	TiCl4 and $AgNO_3$	$AgNO_3$ were reduced by TiO_2 which is irradiated by UV light	Zhao *et al*., 2011
Photo-deposition	$Ti(OBu)_4$ and $AgNO_3$	$AgNO_3$ were reduced by TiO_2 which is irradiated by UV light	Ma *et al*., 2014
Hydrothermal method	TTIP and $AgNO_3$	$AgNO_3$ were reduced by different reductants (ascorbic acid, sodium dodecyl sulphate, NaBH4, Hydrazine, and PEG-600)	Zhang *et al*., 2017
Ultrasonic spray pyrolysis	P25 and $AgNO_3$	Ag nanoparticles were formed by the thermal decomposition of $AgNO_3$	Zhao *et al*., 2012
Flame spray pyrolysis	TTIP and silver benzoate	Ag nanoparticles were formed by the thermal decomposition of $AgNO_3$	Gunawan *et al*., 2009
Sputtering	purity target (Ti and Ag)	Deposition of Ag layer and thermal dewetting (400 °C)	Sanzone *et al*., 2018

Moreover, the reduction of Ag ions to metallic Ag nanoparticles can be classified by 3 routes. One route is using TiO_2 to reduce Ag ions under UV lamp, one route is using reducing agents to reduce Ag ions and one route is the thermal decomposition of silver nitrate. In previous studies, the addition of Ag nanoparticles and Ag ions is considered to have different impacts on the morphological structure and crystalline phase of TiO_2 (Chao *et al.*, 2003； Xin *et al.*, 2005； Mosquera *et al.*, 2016). Therefore, the preparation process which does not involves Ag ions is helpful for the clarification of the role of Ag nanoparticles in photocatalytic reaction.

1.4.2 Effect of annealing temperature on the photocatalytic activity of TiO_2 and Ag-TiO_2

It is well known that heat treatment significantly influences the morphology and crystal structure of TiO_2 materials resulting in a change of photocatalytic activity. Usually, the anatase and rutile phase exhibit great photocatalytic activity. However, the as-prepared TiO_2 nanoparticles are usually amorphous and they generally need to be crystallized by annealing at certain temperature.

Kubo *et al*. investigated the effect of annealing temperature on the crystal structure, porous structure, mechanical strength, and porosity of TiO_2 films (Kubo *et al.*, 2015). Mathews *et al*. reported the effects of annealing temperature on structural, optical and photocatalytic properties of TiO_2. The recrystallization in annealing process (below 600 °C) resulted in the reduction of grain boundaries, higher photo-response,

densification of the films, and increasing surface roughness which are positive factors for photocatalytic activity (Mathews *et al.*, 2009). Lin *et al*. assessed the effect of annealing temperature (300–500 °C) on mineralogical, morphological, optical, and photocatalytic properties of TiO_2 film (Lin *et al.*, 2013). The TiO_2 films showed a slight increase in the grain size and a rapid increase in roughness when the annealing temperature increased. However, the optical indirect band gap showed a slight decrease with increasing annealing temperature. 400 °C is considered as the optimal annealing temperature for TiO_2 film. Chen *et al*. (Chen *et al.*, 2003) investigated effect of annealing temperature (250–900 °C) on the crystallinity of TiO_2 nano powders. As the annealing temperature is increased, the crystallite size and particle of TiO_2 increased while specific surface area decreased.

Researcher have reported that the crystal structure and phase content influenced by annealing temperature (300–700 ºC). The photocatalytic activity of prepared Ag-TiO_2 nanocomposites in the mixture anatase and rutile phase was worse than that of the pure anatase phase (Lee et al., 2005). However, other papers mentioned that the mixture of anatase and rutile phase performs well in comparison of pure anatase or rutile (Zhang *et al.*, 2009； Li *et al.*, 2015).

Table 1.2 The effects of annealing temperature on TiO_2 or Ag-TiO_2 nanocomposites.

Annealing temperature (°C)	**Crystallization temperature / phase transition temperature (°C)**	**The effects of annealing temperature**	**Optimal crystal structure for photocatalyst**	**References**
100–1200	400 / 1000	The particle size and crystalline size of TiO_2 increased with increasing annealing temperature while film thickness and porosity decreased	N/A	Kubo *et al*., 2015
400-600	400 / N/A	The recrystallization in annealing process of TiO_2 film resulted in the reduction of grain boundaries, higher photo-response, densification of the films, and increasing surface roughness	Anatase (600 ℃)	Mathews *et al*., 2009
300–500	400 / N/A	The grain size and roughness of TiO_2 film increased with increasing annealing temperature while the optical indirect band gap showed a slight decrease.	Anatase (400 ℃)	Lin *et al*., 2013
250–900	250 / 600	The crystallite size and particle size of TiO_2 increased with increasing annealing temperature while specific surface area decreased	N/A	Chen *et al*., 2003
300–700	300 / 600	The crystalline size in Ag-TiO_2 film increased with increasing annealing temperature	Anatase (500 ℃)	Lee *et al*., 2005

The effect of annealing temperature on TiO_2 or Ag-TiO_2 nanocomposites was shown in Table 1.2. The crystal structures can be adjusted by changing annealing temperature. The particle size, porosity, crystalline size and band gap of TiO_2 can also be influenced

by different annealing temperatures. There are lots of researches which investigated the effect of annealing temperature on crystal structure, morphology, optical property and photocatalytic activity of TiO_2 but few research on the annealing effect of Ag-TiO_2 nanocomposites. The addition of Ag can not only enhance the photoelectron-hole separation but also influence the phase transition and morphology of TiO_2. Hence, the study on the annealing temperature effect on TiO_2 with additional Ag nanoparticles is helpful to understand the key factors in photocatalytic reactio

1.4.3 Effect of particle size on the photocatalytic activity of TiO_2 and Ag-TiO_2

The particle size of TiO_2 is a significant factor for the photocatalytic activity. Usually, the oxygen molecules, water molecules and pollutants are absorbed on the surface of TiO_2. The larger particle size of TiO_2, the less react area between TiO_2 and absorbed molecules. The photocatalytic activity of TiO_2 also decreases with the increase of particle size. Xu *et al*. studied the effects of particle size (12 nm–49 μm) on photocatalytic property of TiO_2. The photocatalytic activity of TiO_2 increased with the decrease of particle size of TiO_2. The photocatalytic activity of TiO_2 showed a significant increase when the particle size of TiO_2 was less than 30 nm (Xu *et al.*, 1999). The TiO_2 samples with particle size from 15 to 30 nm was applied to test the photocatalytic activity by the photocatalytic degradation of MB solution. The photocatalytic activity of TiO_2 increased with the decrease of particle size, the TiO_2 sample with 15 nm particle size showed the highest photocatalytic activity (Jang *et al.*, 2001). The anatase phase of TiO_2 was prepared by a

sol-gel method (Kočí *et al.*, 2009), the crystalline size of anatase phase was in range of 4.5 to 29 nm. The optimum crystalline size for the photocatalytic activity was 14 nm. Almquist and Biswas prepared TiO_2 (5 to 165 nm) by a flame aerosol process method and discussed the photocatalytic activity of prepared TiO_2 and Degussa P25 in the photocatalytic phenol degradation experiment. The results indicated the optimum particle size was in a range of 25 to 40 nm (Almquist and Biswas, 2002). Base on the previous studies, The TiO_2 nanoparticles with 14–40 nm particle size obtain excellent photocatalytic activity.

Table 1.3 The effects of particle size on the photocatalytic activity of TiO_2.

Materials	Particle size	Optimal particle size	Methods	References
TiO_2	12 nm–49 μm	The photocatalytic activity of TiO_2 showed a significant increase when the particle size of TiO_2 was less than 30 nm. the optimal particle size was 12 nm	Sol-gel method	Xu *et al*., 1999
TiO_2	15–30 nm	The photocatalytic activity of TiO_2 increased with the decrease of particle size, the optimal particle size was 15 nm	Hydrolysis method	Jang *et al*., 2001
TiO_2	4.5–29 nm (crystalline size)	The optimum crystalline size for the photocatalytic activity was 14 nm.	Sol-gel method	Kočí *et al*., 2009
P25/TiO_2	5–165 nm	The optimum particle size was in a range of 25 to 40 nm.	Flame aerosol process	Almquist and Biswas, 2002

The noble metal nanoparticle is considered to enhance the photocatalytic activity of TiO_2. For the same amount of loading noble metal nanoparticle, the smaller loading particle size, the larger contact area between TiO_2 and loading noble metal nanoparticles. Moreover, the loading metal particle size is also considered to influence the electronic properties. When the size of Ag nanoparticle is large, the Ag sites are easy to become recombination centers of photogenerated electrons and holes.

Jiang *et al*. reported the Ag size-dependent Ag-TiO_2 photocatalyst (Jiang *et al.*, 2014). The particle size of loading Ag nanoparticle ranged from 1 to 20 nm, the Ag-TiO_2 photocatalyst with 1 nm particle size showed the highest photocatalytic activity among prepared samples. The effect of size distribution of Ag nanoparticles on photochromic behavior and holographic storage dynamics of Ag-TiO_2 films was studied by Han *et al*. The mean particle size of Ag in prepared Ag-TiO_2 film was 4.39 nm, 6.68 nm and 9.48 nm, respectively. The results showed the Ag-TiO_2 film with Ag nanoparticle in small size performed better than the Ag-TiO_2 film with Ag nanoparticle in large size (Han *et al.*, 2011). Base on the previous studies, the Ag nanoparticle in extremely small size is desirable for the loading of Ag-TiO_2 photocatalytic activity.

1.5 Outline and objectives of this dissertation

The main objectives of this dissertation are: (1) Introduce a new one-step gas-phase deposition process for preparation of Ag-TiO_2 nanoparticulate thin films and evaluate the differences between TiO_2 and Ag-TiO_2 photocatalytic films, (2) Investigate the effect of

annealing temperature on Ag-TiO_2 photocatalytic nanoparticulate thin films, and (3) Investigate the effect of Ag content on Ag-TiO_2 photocatalytic nanoparticulate thin films. Fig. 1.8 shows the schematic representation of this dissertation which is consisted of 5 chapters. The brief of objectives in chapter 2–5 are showed as below.

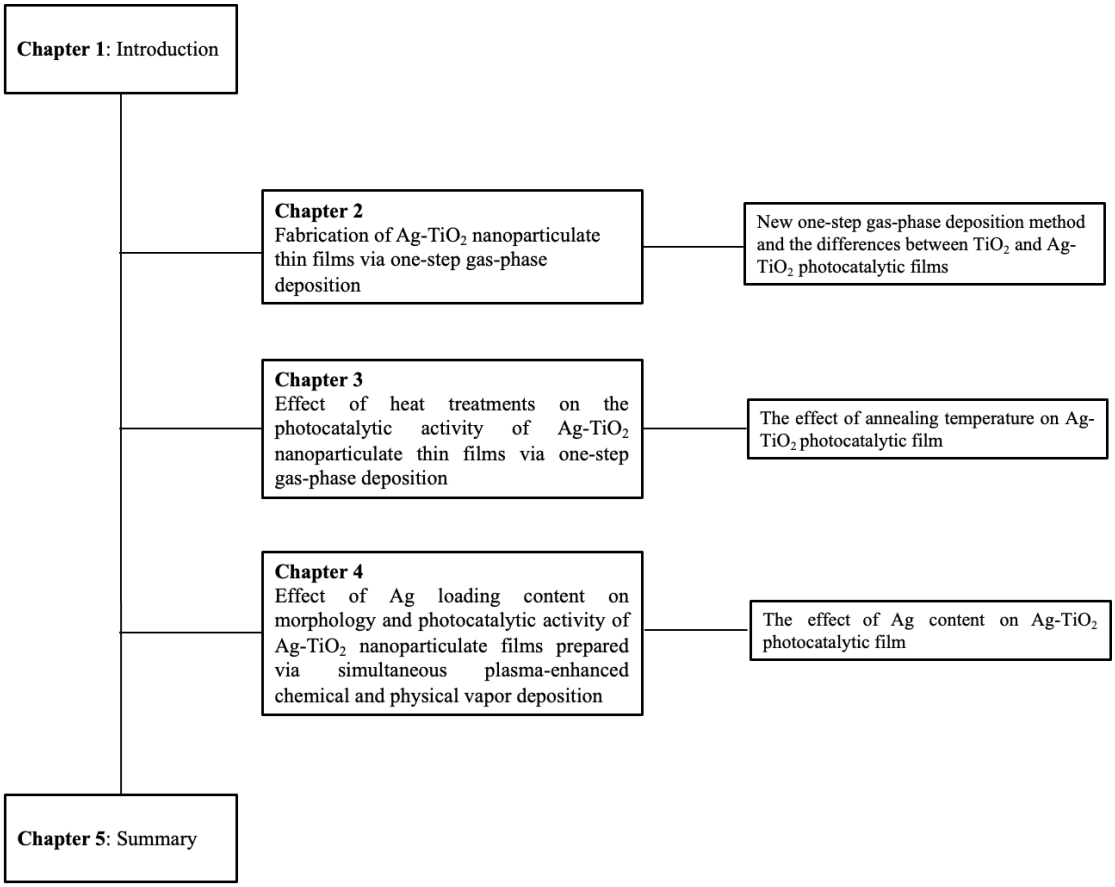

Fig. 1.8 Schematic representation of this dissertation which is consisted of 5 chapters.

It is well known that adding Ag nanoparticles on TiO_2 material enhances the photocatalytic performances. For the fabrication of Ag-TiO_2 nanocomposites, many routes have been used which can be classified as liquid-phase method and gas-phase

method. Generally, the gas-phase methods show advantages such as convenience for preparation and reduced opportunities for contamination and uniform morphological structure of the product. Furthermore, the spray pyrolysis considered as a gas-phase method requires high temperature in preparation of TiO_2 and Ag nanoparticles which leads to particle agglomeration. Moreover, sputtering method need to deposit Ag and Ti layer in molecule level respectively which is hard to control the structure.

To solve the limitations in the reported methods for fabricating Ag-TiO_2 nanoposites, the first objective in chapter 2 is to fabricate non-agglomerated Ag-TiO_2 materials via a efficient, controllable, and solventless process A combination of PECVD technique and PVD technique is applied to fabricate Ag-TiO_2 nanoparticulate film, and the photocatalytic activity will be evaluated base on the morphological analysis, crystal analysis of prepared films.

Moreover, the photocatalytic activity can be influenced by the crystal structure, particle size, lifetime of carriers, loading centration, and the contact area. Previous researches investigated the effect of annealing temperature on crystal structure, morphology, optical property and photocatalytic activity of TiO_2 but few research on the annealing effect of Ag-TiO_2 nanocomposites. The addition of Ag can not only enhance the photoelectron-hole separation but also influence the phase transition and morphology of TiO_2. Hence, the effect of annealing temperature and Ag concentration on the prepared Ag-TiO_2 nanoparticulate film will be evaluated in chapter 3.

Most method prepare Ag nanoparticles by the reduction and thermal decomposition of $AgNO_3$ mixed with TiO_2 precursor or TiO_2. The generation process of Ag nanoparticles is not an independent system which is influenced mutually by the preparation condition of TiO_2. The evaluation of Ag content on photocatalytic activity of Ag-TiO_2 nanocomposites influenced by the mutual effects in preparation of Ag and TiO_2 nanoparticles. The evaluation of Ag content on photocatalytic activity of Ag-TiO_2 nanocomposites prepared by independent Ag and TiO_2 preparation systems is desired

Most of mentioned preparation processes of Ag-TiO_2 nanocomposites involves the reduction of Ag ions. In previous studies, the addition of Ag nanoparticles and Ag ions is considered to have different impact on the morphology and crystal structure of TiO_2.

Despite previous research, the correlation between Ag (especially metallic Ag nanoparticles) and the resulting changes in TiO_2 morphology and phase transition is not well understood. Therefore, the effect of Ag nanoparticle on the photocatalytic activity of Ag-TiO_2 nanoparticulate film will be also investigated base on the morphology, crystal structure and optical property of prepared films in chapter 4.

References

Almquist, C. B. and P. Biswas, "Role of synthesis method and particle size of nanostructured TiO_2 on its photoactivity" *Journal of Catalysis*, **212**, 145-156 (2002).

Avciata, O., Y. Benli, S. Gorduk and O. Koyun, "Ag doped TiO_2 nanoparticles prepared by hydrothermal method and coating of the nanoparticles on the ceramic pellets for photocatalytic study: Surface properties and photoactivity" *Journal of Engineering Technology and Applied Sciences*, **1**, 34-50 (2016).

Chao, H. E., Y. U. Yun, H. U. Xingfang and A. Larbot, "Effect of silver doping on the phase transformation and grain growth of sol-gel titania powder" *Journal of the European Ceramic Society*, **23**, 1457-1464 (2003).

Chen, D., Q. Chen, L. Ge, L. Yin, B. Fan, H. Wang, H. Lu, H. Xu, R. Zhang and G. Shao, "Synthesis and Ag-loading-density-dependent photocatalytic activity of Ag@TiO_2 hybrid nanocrystals" *Applied Surface Science*, **284**, 921-929 (2013).

Chen, Y.-F., C.-Y. Lee, M.-Y. Yeng and H.-T. Chiu, "The effect of calcination temperature on the crystallinity of TiO_2 nanopowders" *Journal of crystal growth*, **247**, 363-370 (2003).

Chowdhury, I. H., S. Ghosh and M. K. Naskar, "Aqueous-based synthesis of mesoporous TiO_2 and Ag–TiO_2 nanopowders for efficient photodegradation of methylene blue" *Ceramics International*, **42**, 2488-2496 (2016).

Fujishima, A. and K. Honda, "Electrochemical photolysis of water at a semiconductor electrode" *nature*, **238**, 37-38 (1972).

Fujishima, A., X. Zhang and D. Tryk, "TiO_2 photocatalysis and related surface phenomena" *Surface Science Reports*, **63**, 515-582 (2008).

Geetha, D., S. Kavitha and P. S. Ramesh, "A novel bio-degradable polymer stabilized Ag/TiO_2 nanocomposites and their catalytic activity on reduction of methylene blue under natural sun light" *Ecotoxicology and environmental safety*, **121**, 126-134 (2015).

Ghorbani, H. R., "A review of methods for synthesis of Al nanoparticles" *Oriental Journal of Chemistry*, **30**, 1941-1949 (2014).

Gomathi Thanga Keerthana, B., T. Solaiyammal, S. Muniyappan and P. Murugakoothan, "Hydrothermal synthesis and characterization of TiO_2 nanostructures prepared using different solvents" *Materials Letters*, **220**, 20-23 (2018).

Gunawan, C., W. Y. Teoh, C. P. Marquis, J. Lifia and R. Amal, "Reversible antimicrobial photoswitching in nanosilver" *Small*, **5**, 341-344 (2009).

Gupta, A. R. and V. Kant, "Research article synthesis, characterization and biomedical applications of nanoparticles, Vijayta Gupta Department of Chemistry, University of Jammu, Jammu-180006, India" *Science International*, **1** (2013).

Halin, D. S. C., M. M. A. B. Abdullah, M. A. A. Mohd Salleh, N. Mahmed and K. Abdul Razak (2018). Synthesis and Characterization of Ag/TiO_2 Thin Film via Sol-Gel Method.

Han, R., X. Zhang, L. Wang, R. Dai and Y. Liu, "Size-dependent photochromism-based holographic storage of Ag/TiO_2 nanocomposite film" *Applied Physics Letters*, **98**, 221905 (2011).

Han, Z., J. Zhang, Y. Yu and W. Cao, "A new anode material of silver photo-deposition on TiO_2 in DSSC" *Materials Letters*, **70**, 193-196 (2012).

Harra, J., J. Mäkitalo, R. Siikanen, M. Virkki, G. Genty, T. Kobayashi, M. Kauranen and J. M. Mäkelä, "Size-controlled aerosol synthesis of silver nanoparticles for plasmonic materials" *Journal of Nanoparticle Research*, **14**, 870 (2012).

Hirakawa, T. and P. V. Kamat, "Charge separation and catalytic activity of Ag@ TiO_2 core− shell composite clusters under UV− irradiation" *Journal of the American Chemical Society*, **127**, 3928-3934 (2005).

Hussein, F. H. and M. A. Shaheed, "Preparation and applications of titanium dioxide and zinc oxide nanoparticles" *J Environ Anal Chem*, **2**, 2380-2391 (2015).

Iravani, S., H. Korbekandi, S. V. Mirmohammadi and B. Zolfaghari, "Synthesis of silver nanoparticles: chemical, physical and biological methods" *Research in pharmaceutical sciences*, **9**, 385 (2014).

Jang, H. D., S.-K. Kim and S.-J. Kim, "Effect of particle size and phase composition of titanium dioxide nanoparticles on the photocatalytic properties" *Journal of Nanoparticle Research*, **3**, 141-147 (2001).

Jiang, Z., Q. Ouyang, B. Peng, Y. Zhang and L. Zan, "Ag size-dependent visible-light-responsive photoactivity of Ag–TiO_2 nanostructure based on surface plasmon resonance" *Journal of Materials Chemistry A*, **2**, 19861-19866 (2014).

Kočí, K., L. Obalová, L. Matějová, D. Plachá, Z. Lacný, J. Jirkovský and O. Šolcová, "Effect of TiO_2 particle size on the photocatalytic reduction of CO_2" *Applied Catalysis B: Environmental*, **89**, 494-502 (2009).

Kruis, F. E., H. Fissan and A. Peled, "Synthesis of nanoparticles in the gas phase for electronic, optical and magnetic applications—a review" *Journal of aerosol science*, **29**, 511-535 (1998).

Kubo, M., Y. Ishihara, Y. Mantani and M. Shimada, "Evaluation of the factors that influence the fabrication of porous thin films by deposition of aerosol nanoparticles" *Chemical Engineering Journal*, **232**, 221-227 (2013).

Kubo, M., Y. Mantani and M. Shimada, "Effects of annealing on the morphology and porosity of porous TiO_2 films fabricated by deposition of aerosol nanoparticles" *Journal of Chemical Engineering of Japan*, **48**, 292-299 (2015).

Lee, M. S., S.-S. Hong and M. Mohseni, "Synthesis of photocatalytic nanosized TiO_2–Ag particles with sol–gel method using reduction agent" *Journal of Molecular Catalysis A: Chemical*, **242**, 135-140 (2005).

Lee, S.-Y. and S.-J. Park, "TiO_2 photocatalyst for water treatment applications" *Journal of Industrial and Engineering Chemistry*, **19**, 1761-1769 (2013).

Li, H., X. Shen, Y. Liu, L. Wang, J. Lei and J. Zhang, "Facile phase control for hydrothermal synthesis of anatase-rutile TiO_2 with enhanced photocatalytic activity" *Journal of Alloys and Compounds*, **646**, 380-386 (2015).

Lin, C. P., H. Chen, A. Nakaruk, P. Koshy and C. C. Sorrell, "Effect of Annealing Temperature on the Photocatalytic Activity of TiO_2 Thin Films" *Energy Procedia*, **34**, 627-636 (2013).

Linic, S., P. Christopher and D. B. Ingram, "Plasmonic-metal nanostructures for efficient conversion of solar to chemical energy" *Nature Materials*, **10**, 911-921 (2011).

Luttrell, T., S. Halpegamage, J. Tao, A. Kramer, E. Sutter and M. Batzill, "Why is anatase a better photocatalyst than rutile?--Model studies on epitaxial TiO_2 films" *Sci Rep*, **4**, 4043 (2014).

Ma, J., X. Guo, Y. Zhang and H. Ge, "Catalytic performance of TiO_2@Ag composites prepared by modified photodeposition method" *Chemical Engineering Journal*, **258**, 247-253 (2014).

Malekshahi Byranvand, M., A. Nemati Kharat, L. Fatholahi and Z. Malekshahi Beiranvand, "A review on synthesis of nano-TiO_2 via different methods" *Journal of nanostructures*, **3**, 1-9 (2013).

Mathews, N. R., E. R. Morales, M. A. Cortés-Jacome and J. A. Toledo Antonio, "TiO_2 thin films – Influence of annealing temperature on structural, optical and photocatalytic properties" *Solar Energy*, **83**, 1499-1508 (2009).

Mosquera, A. A., J. M. Albella, V. Navarro, D. Bhattacharyya and J. L. Endrino, "Effect of silver on the phase transition and wettability of titanium oxide films" *Sci Rep*, **6**, 1-14 (2016).

Nishizawa, J.-I., "Photoassisted deposition process" *Thin Solid Films*, **163**, 149-156 (1988).

Pal, J. and T. Pal, "Faceted metal and metal oxide nanoparticles: design, fabrication and catalysis" *Nanoscale*, **7**, 14159-14190 (2015).

Paz, Y., "Application of TiO_2 Photocatalysis for air Treatment: Patents' Overview" *Applied Catalysis B: Environmental*, **99**, 448-460 (2010).

Pazoki, M., N. Taghavinia, Y. Abdi, F. Tajabadi, G. Boschloo and A. Hagfeldt, "CVD-grown TiO 2 particles as light scattering structures in dye-sensitized solar cells" *RSC Advances*, **2**, 12278-12285 (2012).

Sangpour, P., F. Hashemi and A. Z. Moshfegh, "Photoenhanced degradation of methylene blue on cosputtered M:TiO_2 (M = Au, Ag, Cu) nanocomposite systems: A comparative study" *The Journal of Physical Chemistry C.*, **114**, 13955-13961 (2010).

Sanzone, G., M. Zimbone, G. Cacciato, F. Ruffino, R. Carles, V. Privitera and M. G. Grimaldi, "Ag/TiO_2 nanocomposite for visible light-driven photocatalysis" *Superlattices and Microstructures*, **123**, 394-402 (2018).

Schneider, J., M. Matsuoka, M. Takeuchi, J. Zhang, Y. Horiuchi, M. Anpo and D. W. Bahnemann, "Understanding TiO_2 photocatalysis: mechanisms and materials" *Chemical reviews*, **114**, 9919-9986 (2014).

Sellappan, R., M. G. Nielsen, F. González-Posada, P. C. K. Vesborg, I. Chorkendorff and D. Chakarov, "Effects of plasmon excitation on photocatalytic activity of Ag/TiO_2 and Au/TiO_2 nanocomposites" *Journal of Catalysis*, **307**, 214-221 (2013).

Sun, B., A. V. Vorontsov and P. G. Smirniotis, "Role of platinum deposited on TiO_2 in phenol photocatalytic oxidation" *Langmuir*, **19**, 3151-3156 (2003).

Sung-Suh, H. M., J. R. Choi, H. J. Hah, S. M. Koo and Y. C. Bae, "Comparison of Ag deposition effects on the photocatalytic activity of nanoparticulate TiO_2 under visible and UV light irradiation" *Journal of Photochemistry and Photobiology A: Chemistry*, **163**, 37-44 (2004).

Tan, Y. N., C. L. Wong and A. R. Mohamed, "An Overview on the Photocatalytic Activity of Nano-Doped-TiO_2 in the Degradation of Organic Pollutants" *ISRN Materials Science*, **2011**, 1-18 (2011).

Tang, H., H. Berger, P. E. Schmid, F. Levy and G. Burri, "Photoluminescence in TiO_2 anatase single crystals" *Solid State Communications*, **87**, 847-850 (1993).

Xin, B., L. Jing, Z. Ren, B. Wang and H. Fu, "Effects of simultaneously doped and deposited Ag on the photocatalytic activity and surface states of TiO_2" *The Journal of Physical Chemistry B*, **109**, 2805-2809 (2005).

Xu, N., Z. Shi, Y. Fan, J. Dong, J. Shi and M. Z. C. Hu, "Effects of Particle Size of TiO_2 on Photocatalytic Degradation of Methylene Blue in Aqueous Suspensions" *Industrial & Engineering Chemistry Research*, **38**, 373-379 (1999).

Yu, J., J. Xiong, B. Cheng and S. Liu, "Fabrication and characterization of Ag–TiO_2 multiphase nanocomposite thin films with enhanced photocatalytic activity" *Applied Catalysis B: Environmental*, **60**, 211-221 (2005).

Zhang, H. and G. Chen, "Potent antibacterial activities of Ag/TiO_2 nanocomposite powders synthesized by a one-pot sol− gel method" *Environmental Science & Technology*, **43**, 2905-2910 (2009).

Zhang, X., X. Ge and C. Wang, "Synthesis of titania in ethanol/acetic acid mixture solvents: phase and morphology variations" *Crystal Growth & Design*, **9**, 4301-4307 (2009).

Zhang, Y., T. Wang, M. Zhou, Y. Wang and Z. Zhang, "Hydrothermal preparation of Ag-TiO_2 nanostructures with exposed {001}/{101} facets for enhancing visible light photocatalytic activity" *Ceramics International*, **43**, 3118-3126 (2017).

Zhao, B. and Y.-W. Chen, "Ag/TiO_2 sol prepared by a sol–gel method and its photocatalytic activity" *Journal of Physics and Chemistry of Solids*, **72**, 1312-1318 (2011).

Zhao, C., A. Krall, H. Zhao, Q. Zhang and Y. Li, "Ultrasonic spray pyrolysis synthesis of Ag/TiO_2 nanocomposite photocatalysts for simultaneous H_2 production and CO_2 reduction" *International Journal of Hydrogen Energy*, **37**, 9967-9976 (2012).

Chapter 2

Fabrication of Ag-TiO_2 nanoparticulate thin films via one-step gas-phase deposition

2.1 Introduction

The addition Ag nanoparticles on TiO_2 surface is considered as a popular surface modification method to enhance photocatalytic activity because the Ag nanoparticles increase the lifetime of photogenerated electron-hole pairs (Liang *et al.*, 2011； Kumar *et al.*, 2013； Gao *et al.*, 2015). Usually, The Ag-TiO_2 nanocomposites are prepared by liquid-phase and gas-phase methods. However, commonly used liquid-phase methods that include the sol-gel process (Obalová *et al.*, 2013), microwave-assisted hydrothermal reaction (Suwarnkar *et al.*, 2014), and the photoreduction-thermal treatment (Zhang *et al.*, 2008) have several disadvantages involving complex fabrication steps, long preparation time and residues removal process. While in the gas-phase methods such as ultrasonic spray pyrolysis (Zhao *et al.*, 2012) and flame spray pyrolysis (Gunawan *et al.*, 2009), the agglomeration of nanoparticles is easy to form in the high temperature environment for pyrolysis reaction and deposition.

To solve the limitations of the reported preparation methods for Ag-TiO_2 nanocomposite, the objective of this study is to prepare Ag-TiO_2 nanoparticulate film without particle agglomeration via a simple solventless gas-phase process. In the previous studies, a PECVD method was applied to prepare porous and non-agglomerated TiO_2

films (Kubo *et al.*, 2013； Kubo *et al.*, 2015). The TiO_2 nanoparticles generated in the plasma reactor is negatively charged and hard agglomerate due to electrostatic repulsion force. Moreover, the PVD system with a sequential evaporation and condensation processes is considered as a controllable method to fabricate pure Ag nanoparticles in small particle size (Gromov *et al.*, 2015). The amount and particle size of Ag nanoparticle produced in the sequential evaporation and condensation processes can be easily adjusted by the supplied flow rate or furnace temperature for evaporation.

In this work, a one-step process with PECVD and PVD systems is introduced to fabricate non-agglomerated Ag-TiO_2 nanoparticulate thin films. The effects of additional Ag nanoparticles on the photocatalytic activity of the Ag-TiO_2 nanoparticulate films based on the morphology analysis, crystal analysis will be investigated.

2.2. Experimental

2.2.1 Materials and experimental setup

The experiment setup of combined PECVD and PVD systems is shown in Fig. 2.1. The combined process is consisted of three parts: a PECVD system, a PVD system and a deposition chamber.

In the PVD system, Ag nanoparticles were generated from the processes of evaporation and condensation in sequence. Solid Ag ((Kanto Chemical) in a ceramic crucible were put in a furnace (TMF-300N). By heating the furnace, the Ag can be vaporized above melting point (962 ºC, 1 atm). The Ag vapor generated from the furnace

(1100 ºC) can be transported to a water-cooling system by an argon gas stream, In the cooling system, Ag vapor condensed to form Ag nanoparticles in a rapid cooling rate.

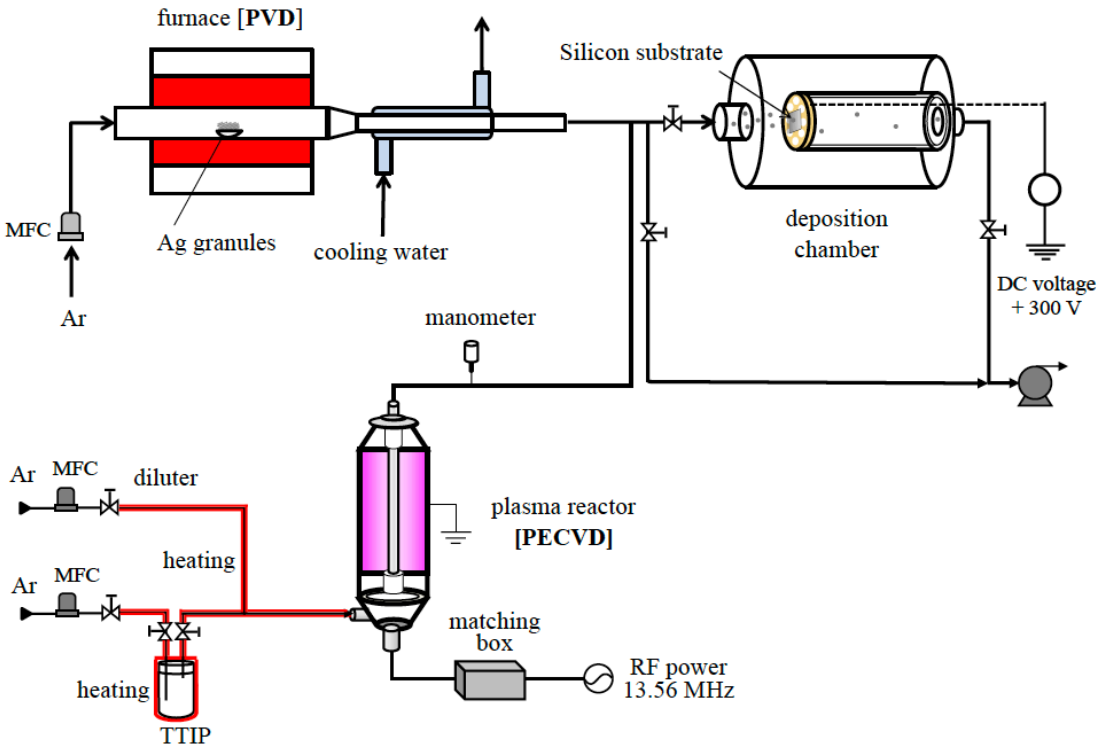

Fig. 2.1 Schematic diagram of the combined PECVD and PVD systems for the fabrication of Ag-TiO_2 nanoparticulate films.

The non-agglomerated TiO_2 nanoparticles were the PECVD system. The precursor of TiO_2, tetraisopropoxide (TTIP) was put into a stainless bubbler. The stainless bubbler was heated at 45 °C and the TTIP became vapor. The carrier gas (argon, 3 sccm) was fed into the heated bubbler and transported the TTIP vapor to the plasma reactor with the diluted argon gas (40 sccm). The TTIP decomposed to TiO_2 nanoparticles after the plasma reaction. The plasma reactor was applied by a RF power supply (100 W, 13.56 MHz, AX-

1000IIP) and a matching network. Heat tapes was used to keep the Ar gas line higher than 45 °C.

The Ag-TiO_2 nanoparticulate films were deposited on a silicon substrate in the deposition chamber. The silicon was applied with a positive voltage of 300 V to get uniform film in a high deposition rate. The deposition time of TiO_2 and Ag-TiO_2 nanoparticulate films was 30 minutes. The as-deposited Ag-TiO_2 nanoparticulate films was put into a furnace for annealing for 12h. The annealing temperature was set at 600 °C.

2.2.2 Characterization

The crystal analysis of the prepared TiO_2 and TiO_2 nanoparticulate thin films were tested by X-ray diffraction (MiniFlex 600, Rigaku, 20°–60°) measurements. Scanning electron microscopy (SEM) and transmission electron microscopy (TEM) were carried out to observe the surface morphology of the prepared Ag-TiO_2 nanoparticulate thin films. EDX was applied to confirm the existence of Ag in the prepared Ag-TiO_2 nanoparticulate thin films.

2.2.3 Photocatalytic test

The photocatalytic degradation of MB aqueous solution was tested under UV irradiation. The prepared Ag-TiO_2 nanoparticulate thin films with mixture of dye solution were put in a dark chamber which was irradiated by a UV lamp (365 nm, 1 W/cm^2). The change of light absorbance in dye solution was tested by the UV-vis spectrophotometry

(V-650, Jasco) which was converted to the change of concentration in dye solution. The photocatalytic degradation processes of MB solution were assumed as first-order reactions. The rate constant (k) in the photocatalytic reaction of the prepared films were evaluated a by using Eq. (2.1):

$$\ln(C_0/C_t) = kt, \quad (2.1)$$

where t, C_0, and C_t stand for the irradiation time, the initial concentration of MB solution, and the concentration of MB solution after irradiation time t, respectively.

2.3 Results and discussion

2.3.1 Crystal structure analysis

Fig. 2.2 shows the XRD patterns of as-deposited TiO_2 film, as-deposited Ag-TiO_2 nanoparticulate film, annealed TiO_2 film and annealed Ag-TiO_2 nanoparticulate film. The peaks in the XRD patterns appeared at 25.4°, 38.3°, and 48.5° correspond to anatase phase. And the diffraction peaks at 27.8, 36.6, 39.3°, 41.7°, and 57.1° are also obviously observed, which correspond to rutile phase.

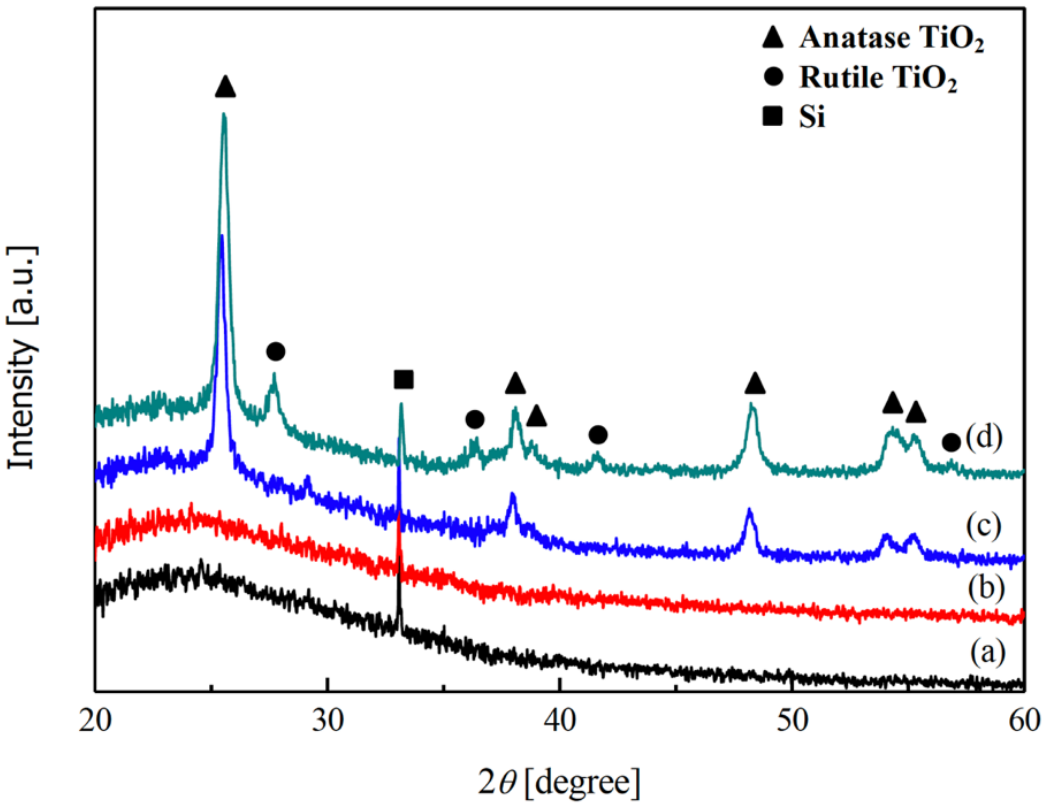

Fig. 2.2 XRD patterns of the pristine TiO_2 film and Ag-TiO_2 nanoparticulate film before and after annealing: (a) as-deposited TiO_2 film, (b) as-deposited Ag-TiO_2 nanoparticulate film, (c) annealed TiO_2 film, and (d) annealed Ag-TiO_2 nanoparticulate film.

2.3.2 Morphological analysis

The top view SEM images of as-deposited pristine TiO_2 and Ag-TiO_2 nanoparticulate films are shown in Fig. 2.3 (a) and (c). The particle size of TiO_2 nanoparticles in as-deposited pristine TiO_2 film showed no big difference with that of Ag-TiO_2 nanoparticulate film. In contrast, the particle size of annealed TiO_2 nanoparticles increased heavily after annealing in comparison with the particle size of TiO_2 nanoparticle in annealed pristine TiO_2 film. In Fig. 2.3(d), the particle size of TiO_2 nanoparticles in

annealed Ag-TiO_2 nanoparticulate film reached to 41 nm while the particle size of annealed TiO_2 nanoparticles in pristine TiO_2 film was only 20 nm which is shown in Fig. 2.3(b). The results showed the existence of Ag nanoparticles help the growth of TiO_2 in the heat treatment. Dehimi *et al*. (Dehimi *et al.*, 2015) also reported the particle size of ZnO was influenced by the addition of Ag in the heat treatment of 500 ºC.

From the SEM images in Fig. 2.3(b) or Fig 2.3(d), It was hard to find Ag nanoparticles because the loading Ag was in a low concentration.

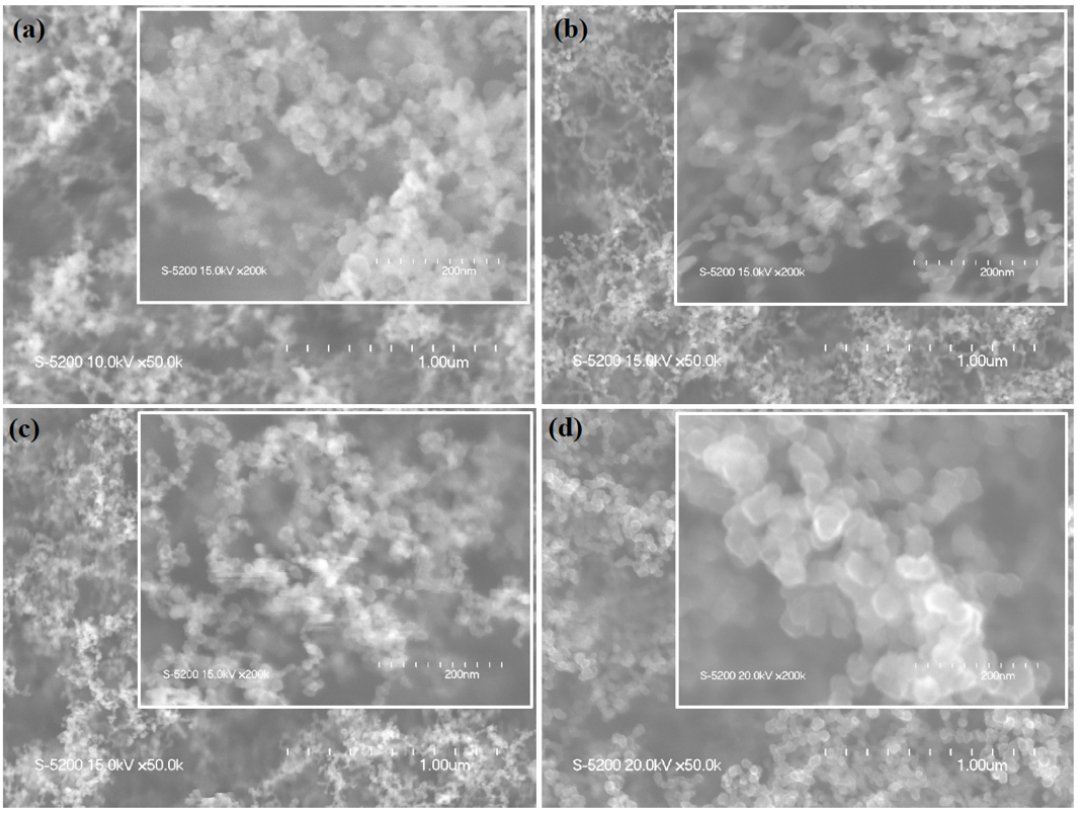

Fig. 2.3 Top view of SEM images of (a) as-deposited TiO_2 film, (b) as-deposited Ag-TiO_2 nanoparticulate film, (c) annealed TiO_2 film, and (d) annealed Ag-TiO_2 nanoparticulate film. The insets are the corresponding SEM images obtained at higher magnifications.

2.3.3 Elemental analysis

Furthermore, the morphology and elemental analysis of Ag-TiO_2 nanocomposites, were measured by high-resolution TEM and EDX techniques (Fig. 2.4). Ag-TiO_2 nanocomposites were deposited on copper grids for 10 seconds with different flow rates of Ag stream supplied to the PVD system. Fig. 2.4 (a) shows the TEM image of the Ag-TiO_2 nanocomposite fabricated at 40 sccm flow rate of Ag stream.

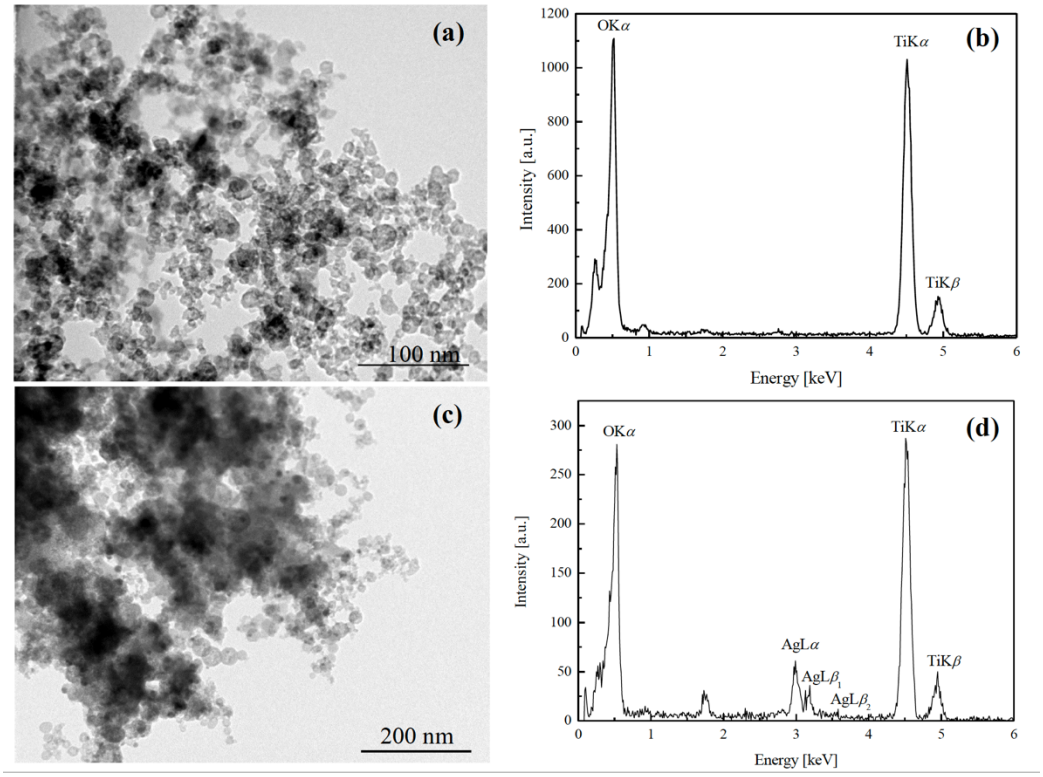

Fig. 2.4 TEM images and EDX spectrum of Ag-TiO_2 nanoparticulate film prepared by different Ag flow rates: 40 sccm ((a) and (b)) and 500 sccm ((c) and (d)), respectively.

Unfortunately, there are only O and Ti peaks appeared at around 0.5 keV and 4.5 keV in the EDX spectrum of Ag-TiO_2 nanoparticulate film prepared by Ag flow rate of 40 sccm in Fig. 2.4 (b). When the Ag flow rate was increased from 40 to 500 sccm, the

peaks of Ag appeared in the EDX spectrum. The appearance of Ag peaks in EDX spectrum can be considered as an evidence that Ag nanoparticles exists in the Ag-TiO_2 nanoparticulate film and the Ag concentration in the prepared films can be easily controlled by changing the Ag flow rate. The increasing gas flow rate shortens the residence time of Ag nanoparticles inside the pipe and increases the cooling rate of Ag vapor. Consequently, a higher number of Ag nanoparticles can be transported and deposited by the gas stream.

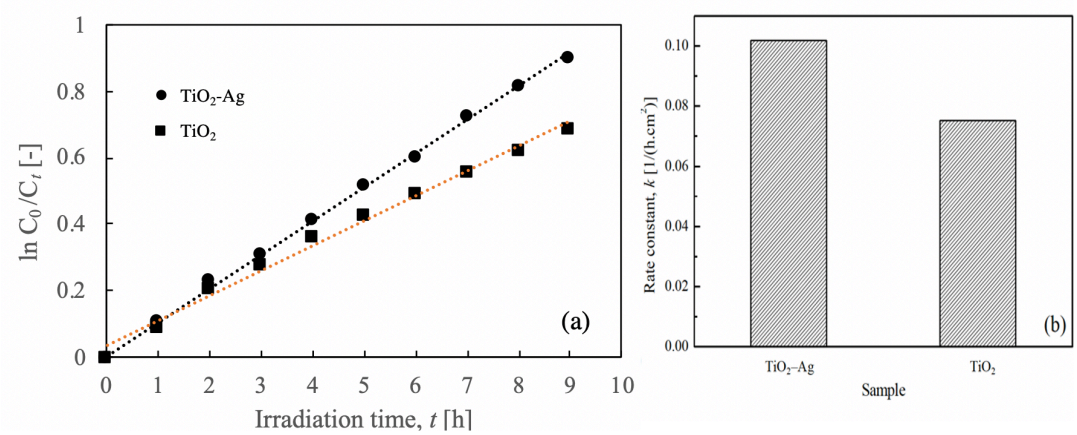

Fig. 2.5 Rate constants (b) of the annealed TiO_2 and Ag-TiO_2 nanoparticulate films calculated by the slope of plots of ln C_0/Ct vs time.

2.3.4 Photocatalytic activities of prepared films

The photocatalytic activities of the annealed TiO_2 and Ag-TiO_2 nanoparticulate films were evaluated by the photocatalytic decolorization of MB aqueous solution irradiated by UV light. The photocatalytic degradation processes of MB solution were assumed as first-order reactions. The rate constants of the annealed TiO_2 and Ag-TiO_2 nanoparticulate films were calculated by the slope of plots of ln C_0/Ct vs time.

The obtained result as shown in Fig 2.5 (b) showed that the photocatalytic activity of the annealed Ag-TiO_2 nanoparticulate film was about 35% greater than the photocatalytic activity of the annealed TiO_2 film. From the Fig 2.5 (a), the calibration curve is not straight, which means the degradation of MB solution was not simply by the photocatalysis. Initially, the degradation rate was fast due the synergic effect of adsorption and the photocatalysis. After the dye molecule got the adsorption equilibrium, the degradation rate became slow.

As we know, the photocatalytic activity can be influenced by a number of integrated factors such as loading concentration of noble nanoparticles, the crystal structure, particle size, lifetime of photogenerated electron-hole pairs, and the contract area (Liu *et al.*, 2004; Sung-Suh *et al.*, 2004; Tan *et al.*, 2011). In this work, the particle size of TiO_2 nanoparticles in Ag-TiO_2 nanoparticulate film was larger than that of TiO_2 nanoparticles in pristine TiO_2 which is a negative factor for photocatalysis. The increase of particle size of TiO_2 nanoparticles led to a decrease in surface area of TiO_2 nanoparticles and therefore decreases its photocatalytic activity. However, the photocatalytic activity of annealed Ag-TiO_2 nanoparticulate film was higher that of annealed TiO_2 film. The reason can be explained by the following two reasons. On one hand, the additional Ag nanoparticles reduce the recommendation of photogenerated electron-hole pairs in TiO_2. The excited electrons in the TiO_2 transfer to the Ag to make the separation of electron-hole pairs. On the other hand, the co-existence of anatase phase and rutile phase can prolong the lifetime of electrons and holes. Yu *et al*. reported that the co-existence of Ag, rutile phase and

anatase phase perform well in the photocatalytic test because this structure can inhibit the recommendation of photogenerated electron-hole pairs (Yu *et al.*, 2005). Therefore, the addition of Ag is the key factor for the photocatalytic activity of Ag-TiO_2 nanoparticulate film as it influenced the particle growth of TiO_2 nanoparticles, the phase transformation in heat treatment, and the separation of electron-hole pairs.

2.4 Conclusions

A new gas-phase process for preparing Ag-TiO_2 nanoparticulate films by a combined PECVD and PVD systems has been successfully developed. The existence of Ag nanoparticles heavily affected the particle size and crystal structure of the prepared Ag-TiO_2 nanoparticulate film. The addition of Ag led to an increase in the particle size and a decrease of phase transition. Comparing with the pristine TiO_2 film, the Ag-TiO_2 nanoparticulate film had a 35% increase in photocatalytic activity based on the photodegradation of MB solution. The addition of Ag is considered as a key factor to influence the photocatalytic activity Ag-TiO_2 nanoparticulate film on the particle size, crystal structure, and the recombination rate of electrons and holes. The mixture of anatase and rutile phases and the addition of Ag are considered as the determined reasons for the increase of photocatalytic activity despite the increasing particle size.

References

Dehimi, M., T. Touam, A. Chelouche, F. Boudjouan, D. Djouadi, J. Solard, A. Fischer, A. Boudrioua and A. Doghmane, "Effects of Low Ag Doping on Physical and Optical

Waveguide Properties of Highly Oriented Sol-Gel ZnO Thin Films" *Advances in Condensed Matter Physics*, **2015**, 1-10 (2015).

Gao, F., Y. Yang and T. Wang, "Preparation of porous TiO_2/Ag heterostructure films with enhanced photocatalytic activity" *Chemical Engineering Journal*, **270**, 418-427 (2015).

Gromov, D. G., L. M. Pavlova, A. I. Savitsky and A. Y. Trifonov, "Nucleation and growth of Ag nanoparticles on amorphous carbon surface from vapor phase formed by vacuum evaporation" *Applied Physics A*, **118**, 1297-1303 (2015).

Gunawan, C., W. Y. Teoh, C. P. Marquis, J. Lifia and R. Amal, "Reversible antimicrobial photoswitching in nanosilver" *Small*, **5**, 341-344 (2009).

Kubo, M., Y. Ishihara, Y. Mantani and M. Shimada, "Evaluation of the factors that influence the fabrication of porous thin films by deposition of aerosol nanoparticles" *Chemical Engineering Journal*, **232**, 221-227 (2013).

Kubo, M., Y. Mantani and M. Shimada, "Effects of annealing on the morphology and porosity of porous TiO_2 films fabricated by deposition of aerosol nanoparticles" *Journal of Chemical Engineering of Japan*, **48**, 292-299 (2015).

Kumar, M., K. K. Parashar, S. K. Tandi, T. Kumar, D. C. Agarwal and A. Pathak, "Fabrication of Ag:TiO_2 nanoocomposite thin films by sol-gel followed by electron beam physical vapour deposition technique" *Journal of Spectroscopy*, **2013**, 1-6 (2013).

Liang, Y.-C., C.-C. Wang, C.-C. Kei, Y.-C. Hsueh, W.-H. Cho and T.-P. Perng, "Photocatalysis of Ag-Loaded TiO_2 Nanotube Arrays Formed by Atomic Layer Deposition" *The Journal of Physical Chemistry C*, **115**, 9498-9502 (2011).

Liu, S., Z. Qu, X. Han and C. Sun, "A mechanism for enhanced photocatalytic activity of silver-loaded titanium dioxide" *Catalysis Today*, **93**, 877-884 (2004).

Obalová, L., M. Reli, J. Lang, V. Matějka, J. Kukutschová, Z. Lacný and K. Kočí, "Photocatalytic decomposition of nitrous oxide using TiO_2 and Ag-TiO_2 nanocomposite thin films" *Catalysis Today*, **209**, 170-175 (2013).

Sung-Suh, H. M., J. R. Choi, H. J. Hah, S. M. Koo and Y. C. Bae, "Comparison of Ag deposition effects on the photocatalytic activity of nanoparticulate TiO_2 under visible and UV light irradiation" *Journal of Photochemistry and Photobiology A: Chemistry*, **163**, 37-44 (2004).

Suwarnkar, M. B., R. S. Dhabbe, A. N. Kadam and K. M. Garadkar, "Enhanced photocatalytic activity of Ag doped TiO_2 nanoparticles synthesized by a microwave assisted method" *Ceramics International*, **40**, 5489-5496 (2014).

Tan, Y. N., C. L. Wong and A. R. Mohamed, "An Overview on the Photocatalytic Activity of Nano-Doped-TiO_2 in the Degradation of Organic Pollutants" *ISRN Materials Science*, **2011**, 1-18 (2011).

Yu, J., J. Xiong, B. Cheng and S. Liu, "Fabrication and characterization of Ag–TiO_2 multiphase nanocomposite thin films with enhanced photocatalytic activity" *Applied Catalysis B: Environmental*, **60**, 211-221 (2005).

Zhang, H., G. Wang, D. Chen, X. Lv and J. Li, "Tuning photoelectrochemical performances of Ag− TiO2 nanocomposites via reduction/oxidation of Ag" *Chemistry of Materials*, **20**, 6543-6549 (2008).

Zhao, C., A. Krall, H. Zhao, Q. Zhang and Y. Li, "Ultrasonic spray pyrolysis synthesis of Ag/TiO_2 nanocomposite photocatalysts for simultaneous H_2 production and CO_2 reduction" *International Journal of Hydrogen Energy*, **37**, 9967-9976 (2012).

Chapter 3

Effect of heat treatments on the photocatalytic activity of Ag-TiO_2 nanoparticulate thin films via one-step gas-phase deposition

3.1 Introduction

It is well known that heat treatment heavily influences the crystal structure and morphology of TiO_2 materials resulting in a change of photocatalytic performance. Generally, amorphous TiO_2 crystallizes to metastable anatase phase in 300–500 ºC annealing temperature and then transform to a stable rutile phase in a higher annealing temperature. Kubo *et al*. used a PECVD method to prepare porous TiO_2 films and investigated the effect of annealing temperature on the morphology and porosity of prepared films (Kubo *et al.*, 2015). The result showed that the annealing temperature had a significant effect on the crystal structure, film thickness, mechanical strength, and porosity of prepared TiO_2 films.

Recent years, Ag-TiO_2 nanocomposites has drawn attention in the photocatalytic filed due to its outstanding property in reduce the recombination rate of photogenerated electron-hole pairs in photocatalytic fields (Lee *et al.*, 2005； Yu *et al.*, 2005； Zhao *et al.*, 2012； Kusdianto *et al.*, 2017). The addition of Ag nanoparticles not only influences the recombination rate of electron-hole pairs, but also affects the morphology and crystal structure of TiO_2. The presence of Ag nanoparticles can also decrease the anatase-to-rutile

phase transition temperature. The Ag-TiO_2 nanocomposites with different annealing temperatures of 300 ºC (Pipelzadeh *et al.*, 2009), 400 ºC (Zhao *et al.*, 2012), 500 ºC (Yu *et al.*, 2005), and 600 ºC (Sangpour *et al.*, 2010) exhibits great photocatalytic activity in comparing with TiO_2.

Furthermore, Researcher have reported that the crystal structure and phase content influenced by annealing temperature (300–700 ºC). The photocatalytic activity of Ag-TiO_2 nanocomposites in the mixture anatase and rutile phase was worse than that of the pure anatase phase (Lee *et al.*, 2005). However, other papers mentioned that the mixture of anatase and rutile phase performs well in comparison of pure anatase or rutile (Zhang *et al.*, 2009； Li *et al.*, 2015). The addition of Ag on the TiO_2 leads to a series of changes in morphology, crystal structure, and electron transfer while the effects of annealing temperature on the morphology and crystal structure is also ignored. Many reports focus on the photocatalytic activity of Ag-TiO_2 nanocomposites analyzed the combined effects of Ag concentration and heat treatment in certain annealing temperature. However, there is a lack of detailed research forcing on the effect of annealing temperature on Ag-TiO_2 nanocomposites or films.

Thus, the effects of annealing temperature on the morphological changes, crystal structure and photocatalytic activity of Ag-TiO_2 nanoparticulate films fabricated via the one-step process with a combination of PECVD and PVD systems will be investigate in this work.

3.2 Experimental

3.2.1 Materials and experimental setup

The experiment setup of combined PECVD and PVD systems. The combined process is consisted of three parts: a PECVD system for the generation of non-agglomerated TiO_2 nanoparticles, a PVD system for the generation of non-agglomerated Ag nanoparticles, and a deposition chamber for the deposition of the Ag-TiO_2 nanoparticulate thin films. The experimental setup for preparing Ag-TiO_2 nanoparticulate thin films has described in chapter 2.

The furnace temperature in PVD system was set at 1100 ºC with a flow rate of 40 sccm Ar gas. The deposition time of Ag-TiO_2 nanoparticulate films was set in range of 25–30 min. The substrates were weighted before and after deposition to obtain the film weight. Ag-TiO_2 nanoparticulate films with similar weight (0.31 mg ± 5%) was selected for heat treatment. The prepared Ag-TiO_2 nanoparticulate films were put in the furnace heated with various annealing temperatures (300–1000 ºC). When the furnace temperature reached to the target annealing temperature, the prepared films stay warm for 12 hours.

3.2.2 Characterization

The crystal structures of the annealed Ag-TiO_2 nanoparticulate films with various annealing temperature were measured by XRD measurement performed in the 20°–60° range. SEM and TEM were carried out to observe the surface morphology of the prepared

Ag-TiO_2 nanoparticulate thin films. The GMDs of the observed nanoparticles in the TEM images were calculated by using Eq. (3.1) (Kubo *et al.*, 2013):

$$\log(\mathrm{GMD}) = \left(\sum_i^n \log d_{\mathrm{p}i}\right)/n\,, \tag{3.1}$$

where n is the number of measured nanoparticles, and d_{pi} is the diameter of i-th nanoparticle.

The average crystallite size (D) was evaluated by the Scherrer's equation as shown in Eq. (3.2):

$$D = \frac{k\,\lambda}{B\cos\theta} \tag{3.2}$$

where k, λ, B, and θ are the constant (Kubo *et al.*, 2015), the wavelength of X-ray source (λ = 0.15418 nm), the full width at half maximum corresponding to XRD peaks, and the peak angle, respectively.

While the phase content of anatase (W_A) and rutile (W_R) in the nanoparticulate films could be calculated according to the previous report as shown in Eqs. 3.3 (a) and 3.3 (b) (Yu *et al.*, 2005):

$$W_{\mathrm{A}} = \frac{K_{\mathrm{A}}A_{\mathrm{A}}}{K_{\mathrm{A}}A_{\mathrm{A}} + A_{\mathrm{R}} + K_{\mathrm{B}}A_{\mathrm{B}}} \tag{3.3 (a)}$$

$$W_{\mathrm{R}} = \frac{A_{\mathrm{R}}}{K_{\mathrm{A}}A_{\mathrm{A}} + A_{\mathrm{R}} + K_{\mathrm{B}}A_{\mathrm{B}}} \tag{3.3 (b)}$$

where A_A, A_R, A_B represent the intensity of anatase, rutile, and brookite, respectively. While K_A and K_B are two coefficients of anatase and brookite the values of which are 0.886 and 2.721, respectively (Yu *et al.*, 2005).

3.2.3 Photocatalytic experiment

The photocatalytic degradation of MB aqueous solution was tested under UV irradiation. The prepared Ag-TiO_2 nanoparticulate thin films with mixture of dye solution were put in a dark chamber which was irradiated by a UV lamp (254 nm, 1 W/cm^2). The change of light absorbance in dye solution was tested by the UV-vis spectrophotometry (V-650, Jasco) which was converted to the change of concentration in dye solution. The photocatalytic degradation processes of MB solution were assumed as first-order reactions. The rate constant (k) in the photocatalytic reaction of the prepared films were evaluated a by using Eq. (3.4):

$$\ln(C_0/C_t) = kt, \tag{3.4}$$

where t, C_0, and C_t stand for the irradiation time, the initial concentration of MB solution, and the concentration of MB solution after irradiation time t, respectively.

3.3 Results and Discussion

3.3.1 Morphological analysis

The SEM images of the annealed Ag-TiO_2 nanoparticulate films which were annealed in the range of 300–1000 ºC are shown in Fig. 3.1. Fig. 3.2 shows the cross-sectional SEM images of Ag-TiO_2 nanoparticulate films with various annealing temperatures (300–1000 ºC).

The particle size of TiO_2 nanoparticles increased with increasing heating temperature, while the film thickness of prepared Ag-TiO_2 nanoparticulate films

decreased as annealing temperature increased. The GMD of Ag-TiO_2 nanoparticulate films based on the top view of SEM images and the relative thickness of Ag-TiO_2 nanoparticulate films based on cross-sectional SEM images were shown in Fig. 3.3. The film thickness decreases significantly from as-deposited film to annealing temperature at 500 ºC, and then gradually decrease with continuing annealing temperature up to 1000 ºC. This is due to densification process as reported in previous study (Kubo *et al.*, 2015). The particle size increased with increasing annealing temperature annealed. It increased slowly from 300 ºC to 700 ºC then decreased quickly from 750 ºC (91 nm) to 1000 ºC (152 nm). Increasing the particle size after annealing is probably due to the rise in the mobility of the nanoparticles in the coalescence process. During or after the transformation to rutile phase, particles were easy to coalesce to become large particles (Kubo *et al.*, 2013).

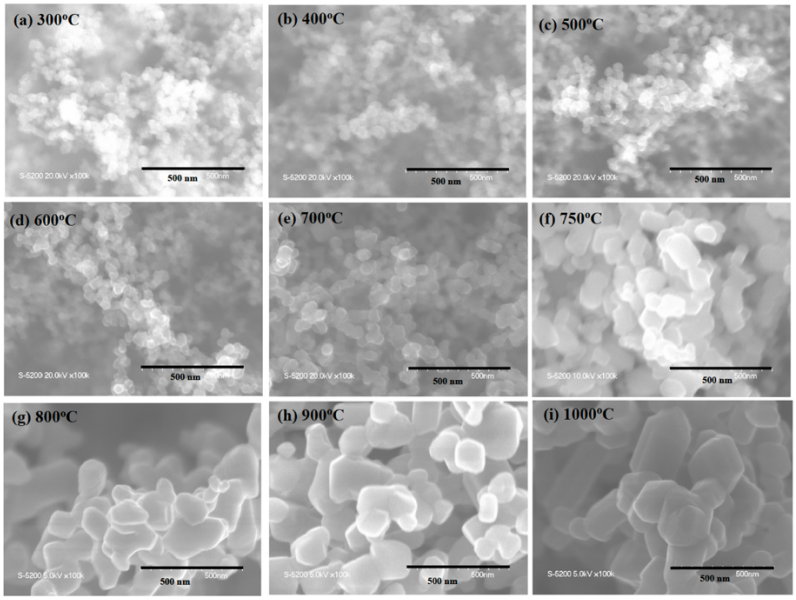

Fig. 3.1 Top view SEM images of Ag-TiO_2 nanoparticulate films with various annealing temperature (300–1000 ºC).

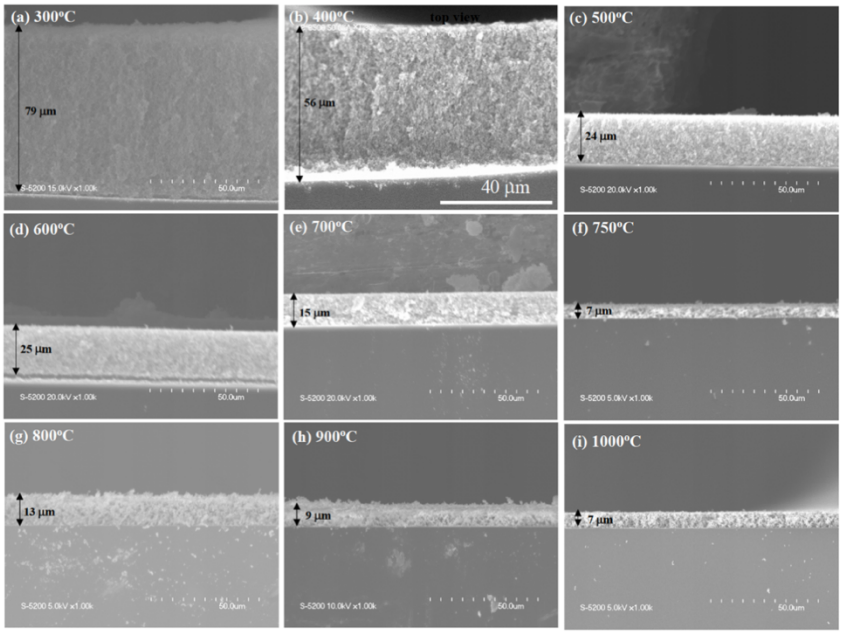

Fig. 3.2 Cross sectional view SEM images of Ag-TiO_2 nanoparticulate films with various annealing temperature (300–1000 ºC).

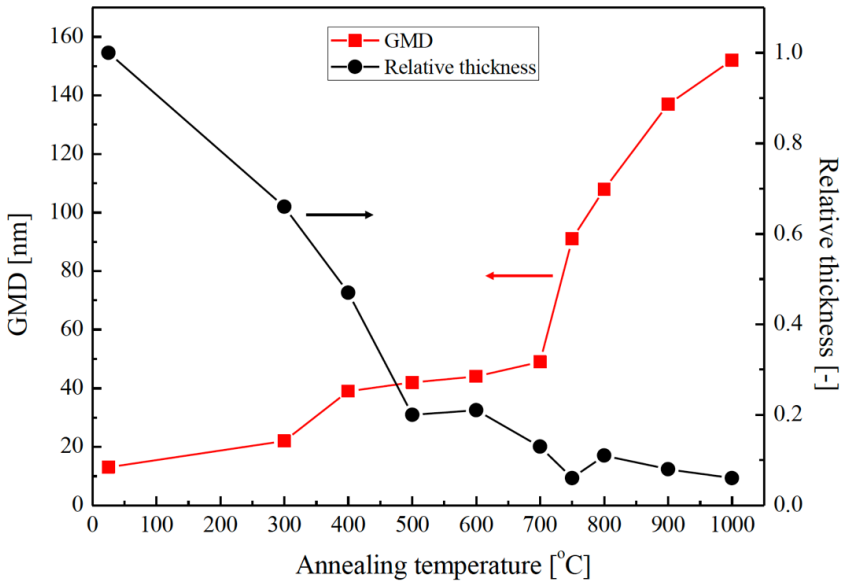

Fig. 3.3 GMD and relative thickness of Ag-TiO_2 nanoparticulate films with various annealing temperature (300–1000 ºC)

3.3.2 Crystal structure analysis

Fig. 3.4 shows the XRD patterns of the prepared Ag-TiO_2 nanoparticulate films with various annealing temperatures (300 to 1000 ºC).

The Ag-TiO_2 nanoparticulate film annealed at 300 ºC did not show any peaks in the XRD pattern. The Ag-TiO_2 nanoparticulate film with 300 ºC annealing was sill amorphous. When the Ag-TiO_2 nanoparticulate film was annealed at 400 ºC, the pure anatase phase appeared in the XRD pattern. It means that the crystallization temperature of TiO_2 started at 400 ºC, which is in a good agreement with the previous work (Kubo *et al.*, 2015) and another work (Wu *et al.*, 2011).When the annealing temperature was in a range from 500 ºC to 800 ºC, the mixture of anatase and rutile phase appeared in the XRD patterns. In the previous study, the phase transition temperature was found at 900 ºC in the TiO_2 fil. But in this study, the phase transition temperature was only about 500 ºC. The result showed that the addition of Ag nanoparticles decreased the phase transition temperature. Similar research (Yu *et al.*, 2005) also reported the presence of Ag nanoparticles accelerated the phase transition from anatase phase to rutile phase. Above the annealing temperature of 800 ºC, only pure rutile phase left in the XRD patterns.

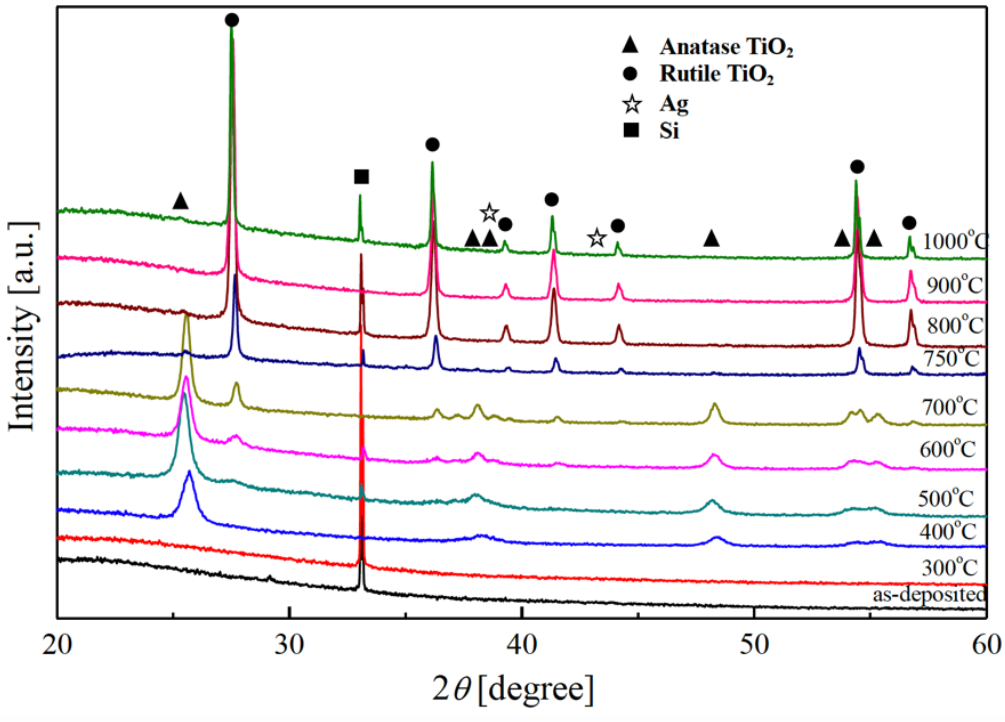

Fig. 3.4 XRD patterns of Ag-TiO_2 nanoparticulate films with the various annealing temperature (300–1000 ºC).

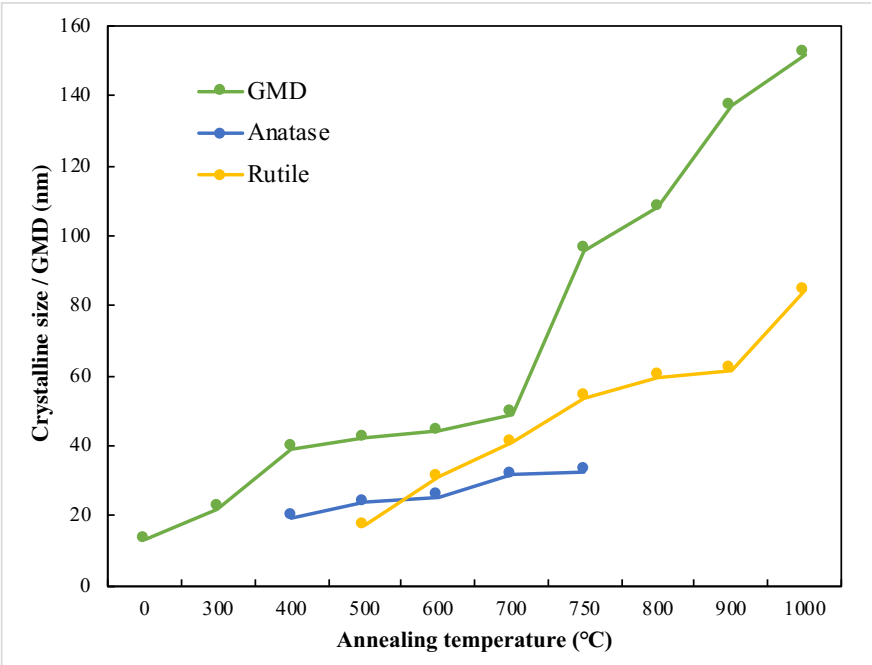

Fig. 3.5 GMD and crystalline sizes of Ag-TiO_2 nanoparticulate films with the various annealing temperature (300–1000 ºC).

Crystalline sizes of Ag-TiO_2 nanoparticulate films with various annealing temperature evaluated by Eq. (3.2) is shown in Fig. 3.5. The crystalline size of both anatase and rutile increased as annealing temperature increased. The anatase nucleus appears in the amorphous TiO_2 and the crystalline size increased with annealing temperature. Subsequently, the rutile phase nucleus occurs in the bulk of anatase phase, and then grows by consuming the anatase phase (Li *et al.*, 2015). The crystalline size of rutile at 500 ºC was smaller than that of anatase, then it becomes larger with increasing annealing temperature. This result in agreement with the proposed phase transition process that the rutile phase generates in the bulk of anatase phase.

The phase content was calculated by using Eq. 3.3 and the result is shown in Fig. 3.6. It shows that the phase content was 100% anatase when the annealing temperature was 400 ºC, then decreases to 8 % after annealed at 750 ºC with increasing annealing temperature. Finally, the phase of anatase completely disappeared when the annealing temperature was raised to 800 ºC. It should be noted that the annealing temperature 700ºC is a key annealing temperature for the crystal structure of prepared Ag-TiO_2 nanoparticulate films. The intensity of anatase phase decreased quickly when the annealing temperature increased from 700 to 750 ºC. Below 700ºC, the majority of crystal structure in the annealed Ag-TiO_2 nanoparticulate films was anatase phase. The majority of crystal structure in the annealed Ag-TiO_2 nanoparticulate films turned into rutile phase when the annealing temperature was above 700 ºC. The dramatic increase of GMD above

700 ºC can be expained by two reasons. One reason is the quick crystal structure change in the short range of 700–750 ºC. The other reason is the increasing crystalline size of rutile above 700 ºC.

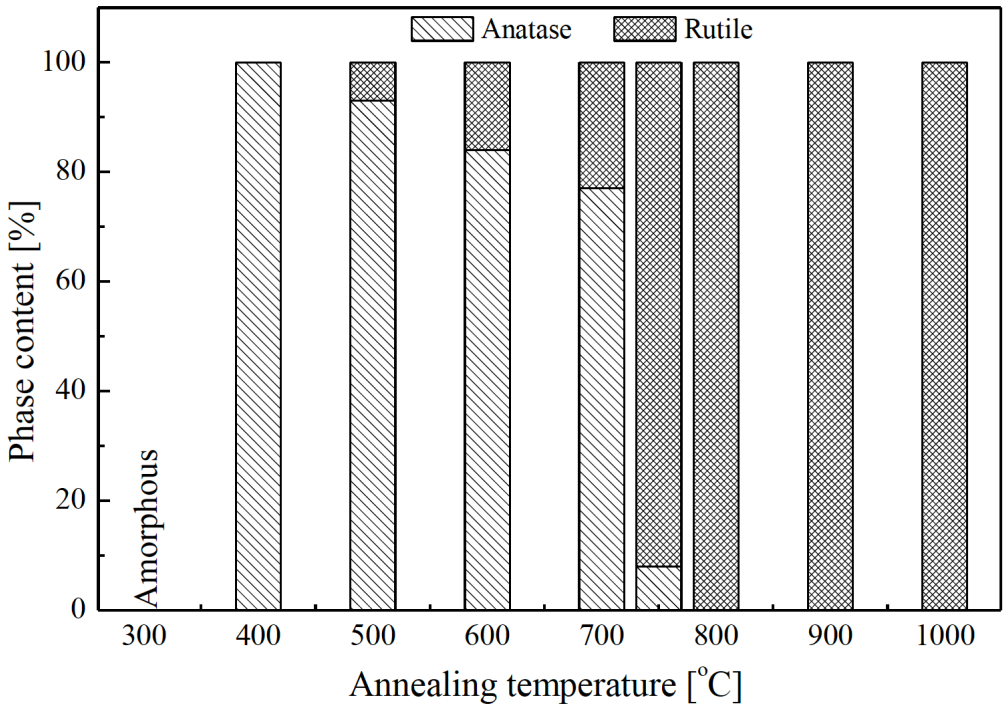

Fig. 3.6 Phase content of anatase and rutile phase in Ag-TiO_2 nanoparticulate films with the various annealing temperature (300–1000 ºC).

3.3.3 Photocatalytic activities of Ag-TiO_2 nanoparticulate films

The photocatalytic activity of Ag-TiO_2 nanoparticulate films with the various annealing temperatures was evaluated by the photocatalytic degradation of MB solution. The rate constant was evaluated by measuring the slope of fitting curves (ln C_0/C_t vs

irradiation time). As shown in Fig. 3.7, the photocatalytic degradation efficiency of MB solution with the Ag-TiO_2 nanoparticulate films at 600 ºC annealing and 700 ºC annealing was higher than the others. In contract, the Ag-TiO_2 nanoparticulate films with annealing temperature above 900 ºC performed worse than other samples in the MB degradation.

Finally, the rate constant of the Ag-TiO_2 nanoparticulate films was measured and the result is shown in Fig. 3.8 including their phase contents. It is obviously observed that the rate constant of the Ag-TiO_2 nanoparticulate film increased significantly and reached to the maximum after annealed at 700 ºC. While the constant decreased drastically in the process of rising temperature from 700 ºC to 1000 ºC. The highest photocatalytic performance was found when the prepared Ag-TiO_2 nanoparticulate film was annealed at 700 ºC. The phase content in the optimal Ag-TiO_2 nanoparticulate film was 77% anatase phase and 23% rutile phase.

The differences in photocatalytic performance of Ag-TiO_2 nanoparticulate films with various annealing temperature can be explained by the combined reasons based on crystalline size, particle size and phase contents, and the electron-hole recombination.

The crystal structure with high crystallinity exhibits good photocatalytic performance where few defects in the crystal structure. The defects in crystal structure is easy to be recombination centers for the photogenerated electron-hole pairs under UV light (Tian *et al.*, 2010). This is the reason that the photocatalytic preformance of samples with anatase phase was better than that of the amorphous sample annealed at 300 ºC.

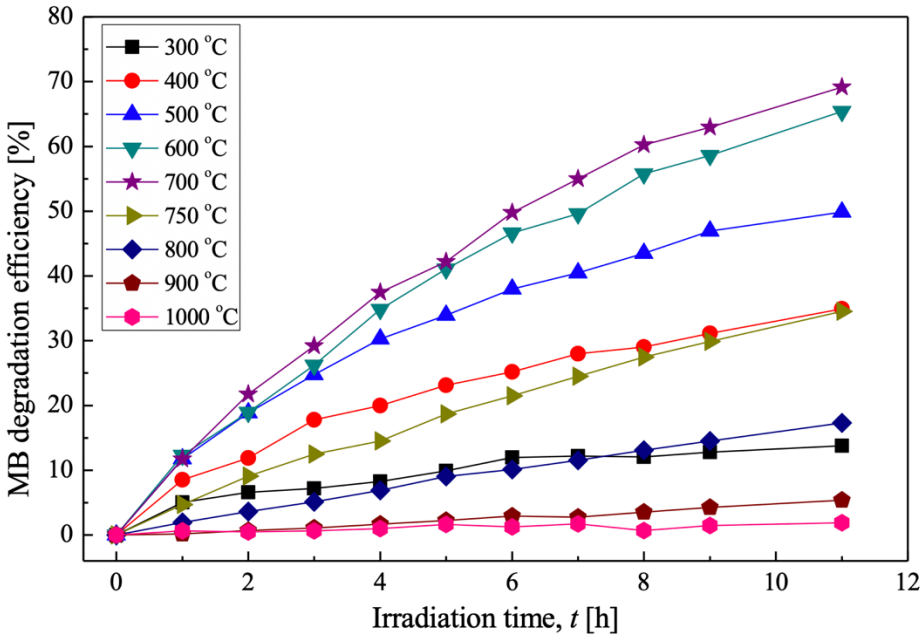

Fig 3.7 Plots of MB degradation efficiency of Ag-TiO_2 nanoparticulate films with the various annealing temperature (300–1000 ºC).

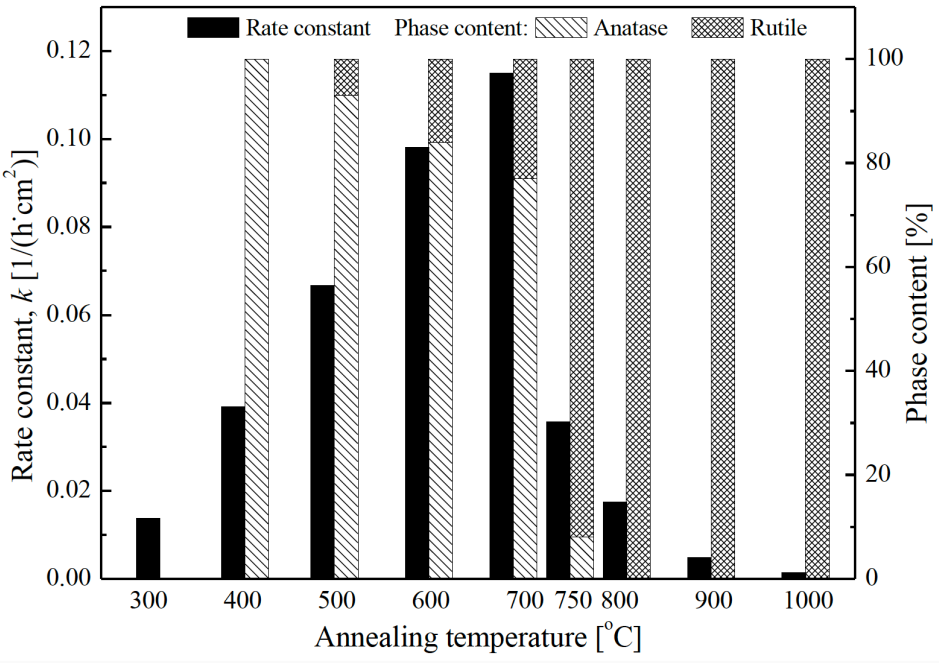

Fig 3.8 The rate constant and phase content of Ag-TiO_2 nanoparticulate films with various annealing temperature (300–1000 ºC).

Photocatalytic performance of anatase phase obtained at 400 ºC was higher than that of rutile phase obtained from 800 to 1000 ºC. It can be explained by the following factors or their combination effects. On one hand, the particles size of anatase are smaller than that of rutile in resulting a higher specific surface area in the prepared Ag-TiO_2 nanoparticulate film. The higher specific surface area is important in photocatalytic reaction because it leads to more active sites to react with absorbed dye molecules. On the other hand, the carrier lifetime in anatase (> 1 μs) is much longer than that of rutile which is efficient to participate in photocatalytic reactions (Yan *et al.*, 2005； Yamada and Kanemitsu, 2012； Luttrell *et al.*, 2014).

While the enhanced photocatalytic performance of the mixed anatase-rutile at temperature in range of 500 to 700 ºC can ascribe to the synergistic effect between anatase phase and rutile phase. Due to the differences in band gap, photogenerated electrons in the anatase phase will transfer into rutile phase, while the generated holes tend to move in the reversed direction (Yan *et al.*, 2005； Li *et al.*, 2015). Therefore, the conbanation of anatase phase and rutile phase can reduce the recombination of electron-hole pairs and increase the lifetime of created electron-hole pairs. The highest photocatalytic activity was found at annealing temperature of 700 ºC, which the produced nanocomposite consists of 77% anatase and 23% rutile. I believe that this composition allows the appropriate condition for the electron and hole transfer during photocatalytic reaction. The obtained optimal ratio of anatase and rutile for photocatalytic activity is in good

agreement with previous studies that a mixture of about 77% anatase phase and 23% rutile phase (Zhang *et al.*, 2009； Li *et al.*, 2015) showed the optimal photocatalytic performance.

The existence of Ag nanoparticles can enhance the separation of electron-hole pairs in the prepared Ag-TiO_2 films because Ag provides a new direction for electron transfer. Ag nanoparticles, acting as an electron accepter, receive the transferring electrons from TiO_2 nanoparticles. Hence, the separation of electron-hole pairs is enhanced not only between anatase and rutile in TiO_2, but also in the interface between TiO_2 and Ag nanoparticles.

3.4 Conclusions

The effects of annealing temperature on crystal structure, morphology and the photocatalytic activity of Ag-TiO_2 nanoparticulate films fabricated via the combined PECVD and PVD systems have been investigated. Both of particle size and crystalline size of TiO_2 increased with increasing annealing temperature while the thickness showed a decrease. As annealing temperature increased, the crystal structure experienced changes from amorphous to anatase to mixture of anatase and rutile to pure rutile. The best photocatalytic activity was found at the annealing temperature of 700 ℃, which includes anatase phase (77%) and rutile phase (23%). Furthermore, the photocatalytic activity of anatase-rutile phase is better than that of pure anatase phase, and the photocatalytic activity of pure anatase phase is better than that of pure rutile phase.

References

Kubo, M., Y. Ishihara, Y. Mantani and M. Shimada, "Evaluation of the factors that influence the fabrication of porous thin films by deposition of aerosol nanoparticles" *Chemical Engineering Journal*, **232**, 221-227 (2013).

Kubo, M., Y. Mantani and M. Shimada, "Effects of annealing on the morphology and porosity of porous TiO_2 films fabricated by deposition of aerosol nanoparticles" *Journal of Chemical Engineering of Japan*, **48**, 292-299 (2015).

Kusdianto, K., D. Jiang, M. Kubo and M. Shimada, "Fabrication of TiO_2-Ag nanocomposite thin films via one-step gas-phase deposition" *Ceramics International*, **43**, 5351-5355 (2017).

Lee, M. S., S.-S. Hong and M. Mohseni, "Synthesis of photocatalytic nanosized TiO_2–Ag particles with sol–gel method using reduction agent" *Journal of Molecular Catalysis A: Chemical*, **242**, 135-140 (2005).

Li, H., X. Shen, Y. Liu, L. Wang, J. Lei and J. Zhang, "Facile phase control for hydrothermal synthesis of anatase-rutile TiO_2 with enhanced photocatalytic activity" *Journal of Alloys and Compounds*, **646**, 380-386 (2015).

Luttrell, T., S. Halpegamage, J. Tao, A. Kramer, E. Sutter and M. Batzill, "Why is anatase a better photocatalyst than rutile--Model studies on epitaxial TiO_2 films" *Sci Rep*, **4**, 4043 (2014).

Pipelzadeh, E., A. A. Babaluo, M. Haghighi, A. Tavakoli, M. V. Derakhshan and A. K. Behnami, "Silver doping on TiO_2 nanoparticles using a sacrificial acid and its photocatalytic performance under medium pressure mercury UV lamp" *Chemical Engineering Journal*, **155**, 660-665 (2009).

Sangpour, P., F. Hashemi and A. Z. Moshfegh, "Photoenhanced degradation of methylene blue on cosputtered M:TiO_2 (M = Au, Ag, Cu) nanocomposite systems: A comparative study" *The Journal of Physical Chemistry C.*, **114**, 13955-13961 (2010).

Tian, S., H. Yang, M. Cui, R. Shi, H. Zhao, X. Wang, X. Wang and L. Zhang, "Monodisperse rutile TiO_2 nanorod-based microspheres with various diameters: hydrothermal synthesis, formation mechanism and diameter- and crystallinity-dependent photocatalytic properties" *Applied Physics A*, **104**, 149-158 (2010).

Wu, C.-Y., B.-S. Chiang, S. Chang and D.-S. Liu, "Determination of photocatalytic activity in amorphous and crystalline titanium oxide films prepared using plasma-enhanced chemical vapor deposition" *Applied Surface Science*, **257**, 1893-1897 (2011).

Yamada, Y. and Y. Kanemitsu, "Determination of electron and hole lifetimes of rutile and anatase TiO_2 single crystals" *Applied Physics Letters*, **101**, 133907 (2012).

Yan, M., F. Chen, J. Zhang and M. Anpo, "Preparation of controllable crystalline titania and study on the photocatalytic properties" *The Journal of Physical Chemistry B*, **109**, 8673-8678 (2005).

Yu, J., J. Xiong, B. Cheng and S. Liu, "Fabrication and characterization of Ag–TiO_2 multiphase nanocomposite thin films with enhanced photocatalytic activity" *Applied Catalysis B: Environmental*, **60**, 211-221 (2005).

Zhang, X., X. Ge and C. Wang, "Synthesis of titania in ethanol/acetic acid mixture solvents: phase and morphology variations" *Crystal Growth & Design*, **9**, 4301-4307 (2009).

Zhao, C., A. Krall, H. Zhao, Q. Zhang and Y. Li, "Ultrasonic spray pyrolysis synthesis of Ag/TiO_2 nanocomposite photocatalysts for simultaneous H_2 production and CO_2 reduction" *International Journal of Hydrogen Energy*, **37**, 9967-9976 (2012).

Chapter 4

Effect of Ag loading content on morphology and photocatalytic activity of Ag-TiO_2 nanoparticulate films prepared via simultaneous plasma-enhanced chemical and physical vapor deposition

4.1 Introduction

TiO_2, as a promising photocatalyst, has been the object of extensive investigation in recent years due to its excellent property in air and water purification. The loading Ag nanoparticles on the surface of TiO_2 nanoparticles is considered as an effective method to enhance the photocatalytic property of TiO_2 by inhibiting the recombination of photogenerated carriers and broaden the light absorbance spectrum from UV region to visible region.

Various routes have been approached to prepare Ag-TiO_2 nanocomposites including liquid-phase methods and gas-phase methods. The liquid-phase methods such as sol-gel process (He *et al.*, 2002), microwave-assisted hydrothermal reaction (Suwarnkar *et al.*, 2014), and the photoreduction-thermal treatment (Zhang *et al.*, 2008) has been appied to fabricate Ag-TiO_2 films. In addition, ultrasonic spray pyrolysis (Zhao *et al.*, 2012) and flame spray pyrolysis (Gunawan *et al.*, 2009) which can be categorized into gas-phase method. Most of the preparation process mentioned above contain the reduction process of Ag ions. Zhang *et al* used the photoreduction method to reduce the Ag ions to Ag

nanoparticles by mixture with TiO_2 under UV light irradiation. Some researchers used some reducing agents to change the change the chemical state of Ag (Hirakawa and Kamat, 2005). Moreover, the thermal decomposition from silver nitrate was also a popular route to obtain Ag nanoparticles (Wang *et al.*, 2009； Zhao *et al.*, 2012). Zhang *et al* used the photoreduction method that reduce the Ag ions.

In previous studies, the doping of Ag is considered to have an impact on the morphology and crystal structure and the resulting photocatalytic performance of TiO_2. Some researchers have reported that the diffusion and agglomeration of Ag influenced the morphology and anatase-to-rutile transition (He *et al.*, 2002； Yu *et al.*, 2005) by inhibiting the phase growth of anatase. The oxygen vacancies can generate in the TiO_2 due to the doping of Ag. The phase transition from anatase phase to rutile phase occur easily when the oxygen vacancies generated in TiO_2 matrix (Chao *et al.*, 2003； Xin *et al.*, 2005； Mosquera *et al.*, 2016).

Usually, the reduced Ag nanoparticles are deposited on the surface of TiO_2 nanoparticles which is well-crystallized. So the loading Ag showed no obvious impact on the crystal structure and morphology of TiO_2 (Tan *et al.*, 2003； You *et al.*, 2005； Zhang *et al.*, 2008； Chen *et al.*, 2013).While, in the previous research (García-Serrano *et al.*, 2009), The effect on the phase transformation of TiO_2 influenced by the chemical state of Ag where Ag-TiO_2 nanocomposites were annealed at air and nitrogen atmosphere, respectively. Therefore, despite previous research, the effect of Ag (especially metallic Ag nanoparticles) on the morphology and phase transition of TiO_2 is not very clear.

In this work, I introduced a combined PECVD and PVD methods to fabricate the Ag-TiO_2 nanoparticulate films without involving Ag ions in any steps of preparation. And the effects of the Ag content on the photocatalytic activity of Ag-TiO_2 nanoparticulate films were investigated based on the morphological analysis, crystal analysis, elemental analysis and optical analysis.

4.2 Experimental

4.2.1 Materials and experimental set-up

The Ag-TiO_2 nanoparticulate thin films were prepared by the one-step deposition method introduced in chapter 2. The Ag nanoparticles are prepared by the condensation of Ag vapor in the PVD system. In this work, the furnace temperature in PVD system was varied and the Ag amount can be controlled by the amount of Ag vapor in different furnace temperature (25–1200 ℃). The mixed Ag and TiO_2 nanoparticles were deposited for 30 minutes on the silicon substrate with a positive voltage of 500 V. After that, the prepared Ag-TiO_2 nanoparticulate thin films were annealed at 500 ℃ in N_2 annealing environment for 3 hours. A digital lab scale (MSA6.6S0TRDM01; Sartorius) was used to test the weight of prepared films before and after film deposition. All prepared films in a weight of 0.07 mg (± 5%) were chose to measure the photocatalytic activity based on the photocatalytic degradation of MB solution under UV light. Moreover, the photocatalytic degradation of rhodamine 6G (R6G) solution under visible light was also measured with the existence of Ag-TiO_2 nanoparticulate thin films with different Ag content.

4.2.2 Characterization

The crystal analysis of the prepared Ag-TiO_2 nanoparticulate thin films were tested by X-ray diffraction (MiniFlex 600, Rigaku, 20°–60°) measurements. SEM and TEM were carried out to observe the surface morphology of the prepared Ag-TiO_2 nanoparticulate thin films. EDX was applied to confirm the existence of Ag in the prepared Ag-TiO_2 nanoparticulate thin films. The GMDs of the observed nanoparticles in the TEM images were calculated by using Eq. (4.1) (Kubo *et al.*, 2013):

$$\log(\mathrm{GMD}) = \left(\sum_i^n \log d_{\mathrm{p}i}\right)/n\,, \tag{4.1}$$

where n is the number of measured nanoparticles, and $d_{\mathrm{p}i}$ is the diameter of i-th nanoparticle.

The Ag content in the prepared Ag-TiO_2 nanoparticulate thin films were measured by the inductively coupled plasma optical emission spectrometry (ICP-OES). The nitric acid solution (3 ml) was introduced to dissolve the Ag nanoparticles in the prepared Ag-TiO_2 nanoparticulate thin films. The prepared solution involving Ag ions and TiO_2 nanoparticles was filtered by a filter (0.45 μm) and the Ag amount was measured by ICP-OES. The mass concentrations of Ag (mg/L) in the prepared solution were calculated based on the calibration curve of prepared Ag solution (0 to 10 mg/L). And then, the Ag content (ω) in the Ag-TiO_2 nanoparticulate thin films were calculated by using Eq. (4.2):

$$\omega = \rho V/m, \tag{4.2}$$

where ρ is the mass concentration of Ag tested from ICP-OES, V is the volume of nitric acid solution, and m is the weight of the annealed Ag-TiO_2 nanoparticulate thin film.

4.2.3 Photocatalytic experiment

The photocatalytic degradation of MB and R6G aqueous solution were tested under UV irradiation and visible light irradiation, respectively. The prepared Ag-TiO_2 nanoparticulate thin films with mixture of dye solution were put in a dark chamber which was irradiated by a UV lamp (365 nm, 1 W/cm^2) or a xenon light source (385-1000nm, 75mW/cm^2. HAL-C100). The change of light absorbance in dye solution was tested by the UV-vis spectrophotometry (V-650, Jasco) which was converted to the change of concentration in dye solution. The photocatalytic degradation processes of MB and R6G were assumed as first-order reactions. The rate constant (k) in the photocatalytic reaction of the prepared films were evaluated a by using Eq. (4.3):

$$\ln(C_0/C_t) = kt, \tag{4.3}$$

where t, C_0, and C_t stand for the irradiation time, the initial concentration of dye solution (MB or R6G), and the concentration of dye solution (MB or R6G) after irradiation time t, respectively.

4.3. Results and discussion

4.3.1 Crystal structure analysis

Fig. 4.1 shows the crystal analysis results of the annealed pure TiO_2 film and annealed Ag-TiO_2 nanoparticulate thin films with various Ag contents. The Ag content in Ag-TiO_2 nanoparticulate thin films was in a range of 0.5 wt% to 7.4 wt%. From the characteristic peaks at 25.4°, 38.3°, and 48.5° in XRD patterns, the existence of anatase

phase of TiO_2 can be confirmed. No other crystal phases of TiO_2 nor characteristic Ag peaks were found in the diffraction patterns. From the Scherrer's equation, smaller crystallite size contributes to broader peaks in XRD patterns. Hence, the small Ag nanoparticles in Ag-TiO_2 nanoparticulate films are hard to detected. Moreover, the low concentration of Ag is considered as an additive reason for weak signals of Ag in the diffraction patterns. Researchers (Zhang *et al.*, 2011； Zhang *et al.*, 2012) have reported the similar phenomenon that gold nanoparticles in a range of 5 nm–10 nm is difficult to observe in XRD patterns due to extremely small particle size.

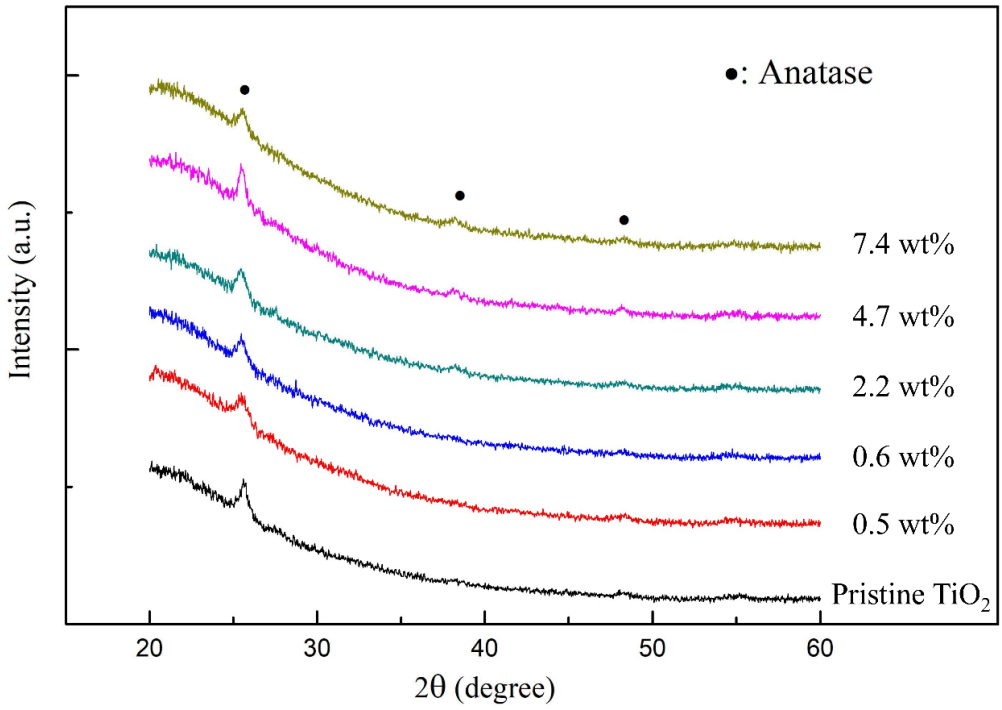

Fig. 4.1 XRD patterns of the annealed TiO_2 film and annealed Ag-TiO_2 nanoparticulate films with various Ag concentrations (0.5–7.4 wt%).

4.3.2 Morphological and elemental analysis

Surface morphologies of the prepared pure TiO_2 film and Ag-TiO_2 films were investigated by SEM. Fig. 4.2 shows the SEM images of the annealed TiO_2 and Ag-TiO_2 films with various Ag concentrations. The porous matrix by the connection of TiO_2 nanoparticles can be observed in the pure TiO_2 and Ag-TiO_2 nanoparticulate films. And the porosity of prepared films is not influence by varying Ag concentration. The porous structure is suitable for the photocatalytic reaction because it can provide a lot of contact area between TiO_2 and other reactants.

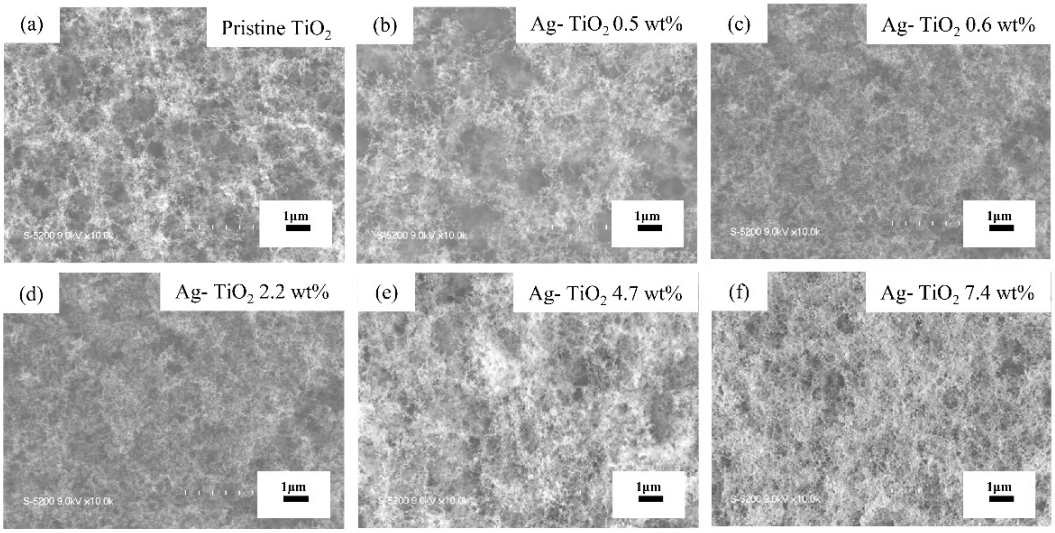

Fig. 4.2 SEM images of the annealed TiO_2 and Ag-TiO_2 films with various Ag concentrations (0.5–7.4 wt%).

The Ag nanoparticles were fabricated by different furnace temperatures (1000 °C, 1150 °C, and 1200 °C) in PVD system and deposited on the copper grid for 10 seconds. The TEM images of prepared Ag nanoparticles at various furnace temperature was shown in Fig. 4.3(a)–(c). The dark and spherical spots which represent Ag nanoparticles can be

clearly observed in the TEM images. The number density of Ag nanoparticles (below 5 nm) also increased with the increasing furnace temperature in the PVD system.

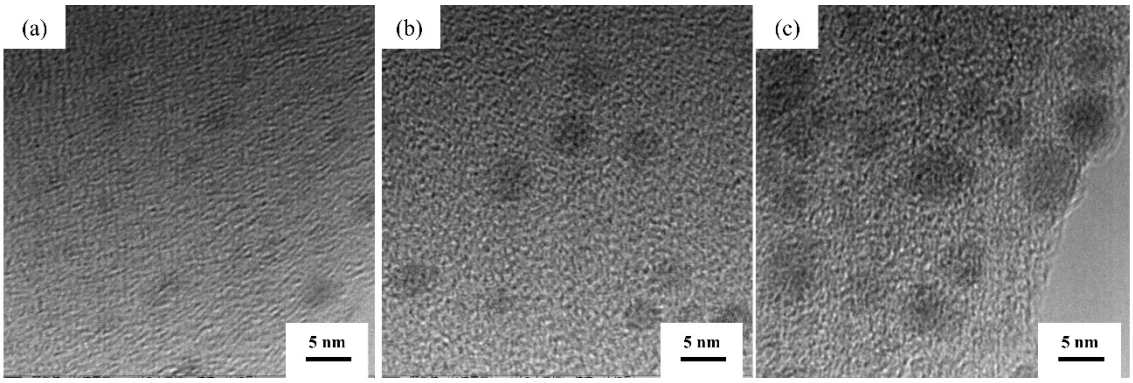

Fig. 4.3 TEM images of deposited Ag nanoparticles on the copper grid obtained by various furnace temperatures (1000 °C, 1150 °C and 1200 °C).

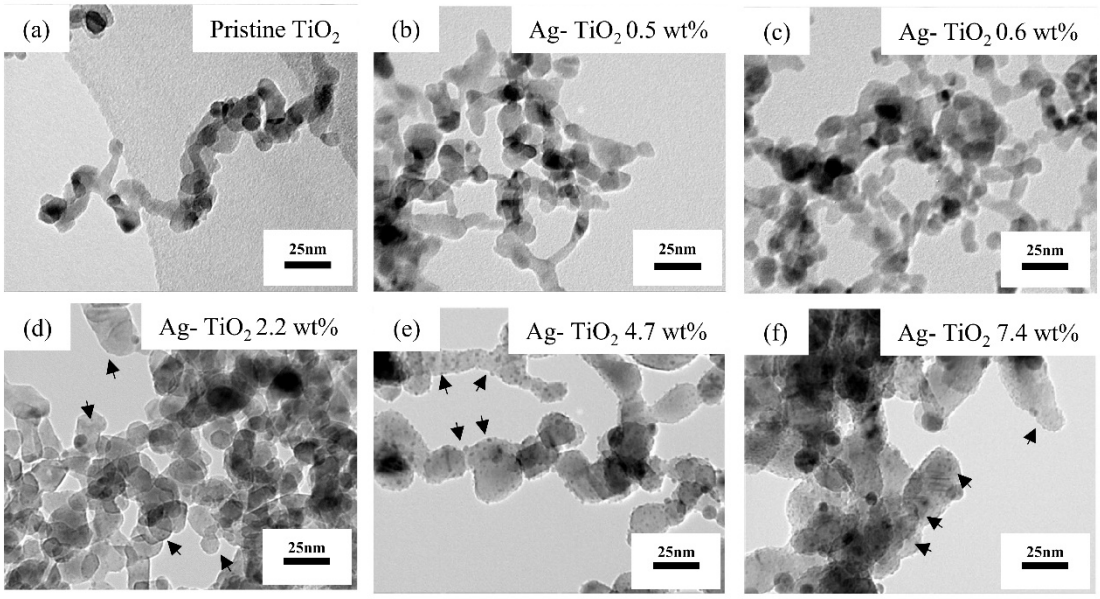

Fig. 4.4 TEM images of the annealed TiO_2 and Ag-TiO_2 films with various Ag concentrations (0.5–7.4 wt%).

Moreover, the differences in the particle size and the morphology of the annealed TiO_2 and annealed Ag-TiO_2 films with various Ag concentrations were observed by TEM and the obtained TEM images are shown in Fig. 4.4. In Fig. 4.4(a), the fiber-like TiO_2 matrix was formed by the connection of annealed TiO_2 nanoparticles. The morphology of fabricated TiO_2 and Ag-TiO_2 films with Ag concentration below 2.2 wt% showed no obvious differences. However, the dark spots appeared in the matrix of TiO_2 when the Ag concentration was above 2.2 wt%. And the number density of these dark spots increased with Ag concentration from 2.2 wt% to 7.4 wt%. These dark spots were considered as Ag nanoparticles which were below 2 nm. Because of the small particle size of Ag nanoparticles and the uniform dispersion, it is hard to detect the peaks of Ag in the XRD patterns.

Further elemental analysis of prepared annealed TiO_2 and Ag-TiO_2 nanoparticulate thin films were measured by the EDX which is combined with TEM. The EDX spectrum of annealed TiO_2 and Ag-TiO_2 nanoparticulate thin films is shown in Fig. 4.5. In Fig. 4.5(a), only the characteristic peaks of Ti and O can be detected. However, the peaks of Ag (at around 3 keV) appeared in the EDX spectrum of the annealed Ag-TiO_2 nanoparticulate film. This result confirmed the existence of Ag in the annealed Ag-TiO_2 nanoparticulate film with an Ag concentration of 7.4 wt%.

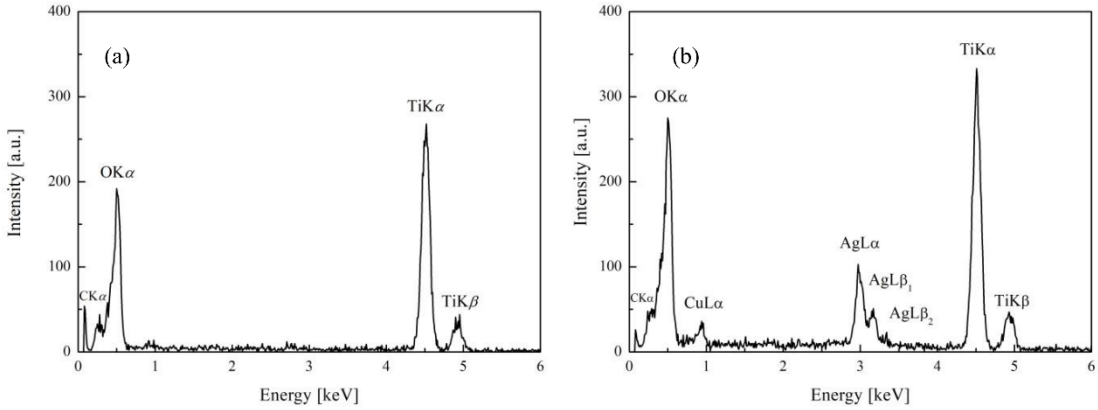

Fig. 4.5 Elemental analysis of annealed TiO_2 and annealed Ag-TiO_2 film with an Ag concentration of 7.4 wt%.

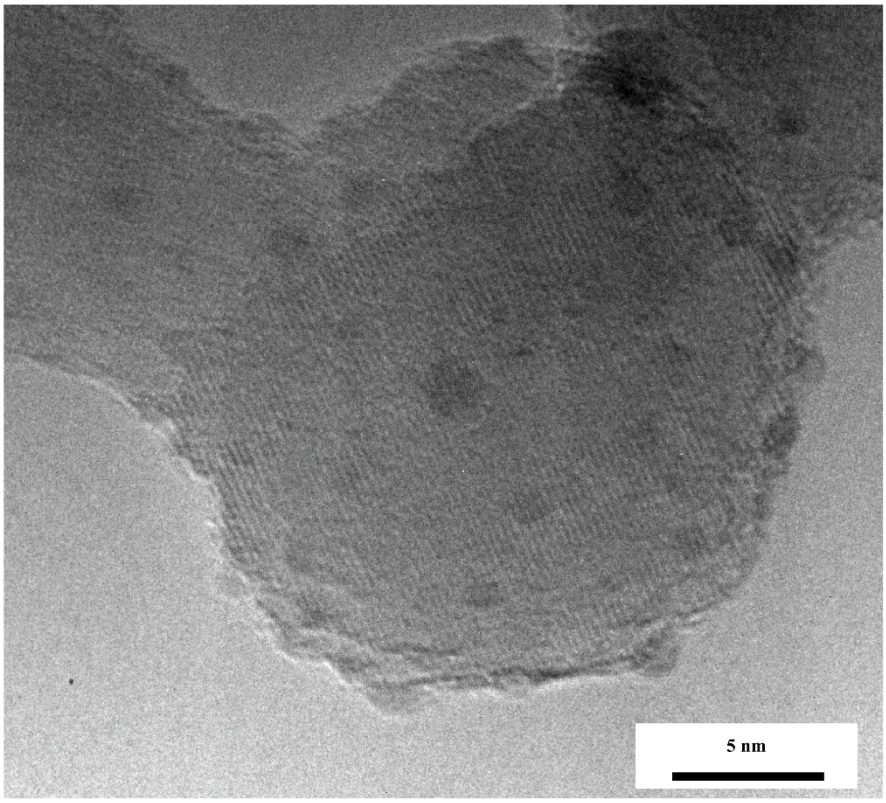

Fig. 4.6 High-resolution TEM image of the prepared Ag-TiO_2 nanocomposite.

The TEM image of the Ag-TiO_2 nanocomposite in the Ag-TiO_2 nanoparticulate film (7.4 wt% Ag) is shown in Fig. 4.6. The Ag nanoparticles (below 3 nm) well dispersed and tightly attached on the surface of the TiO_2 nanoparticles (about 25 nm).

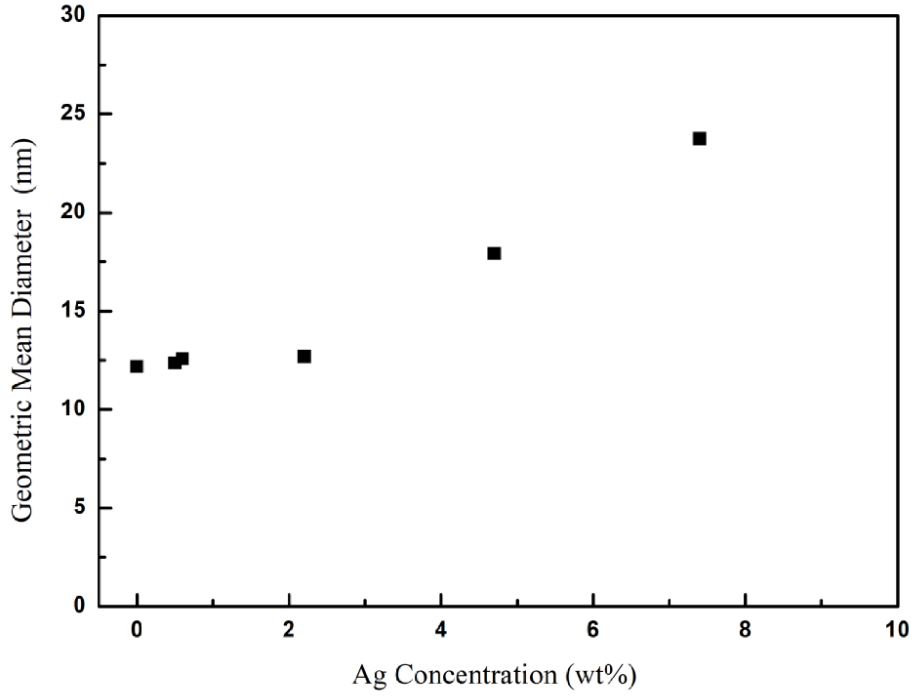

Fig. 4.7 The GMDs of annealed TiO_2 and Ag-TiO_2 nanoparticulate films with various Ag concentration.

Fig. 4.7 shows the GMDs of annealed TiO_2 and Ag-TiO_2 nanoparticulate films with various Ag concentration. The GMDs showed a slight increase when the Ag concentration was below 2.2 wt% and a significant increase when the Ag concentration was above 2.2 wt%. The phenomenon that the additional Ag nanoparticles affect the particle size of TiO_2 has been introduced in chapter 2. Similarly, Dehimi *et al*. also reported that the particle size of ZnO influenced by the added Ag and it increased with

increasing Ag concentration up to 0.5 at.% (Dehimi *et al.*, 2015). Moreover, In previous study the anatase grain size increased with increasing Ag dopant concentration in the Ag-TiO_2 nanocomposites (He *et al.*, 2002). Therefore, the existence of Ag nanoparticles in the TiO_2 matrix is considered to be a positive factor for the crystallization of TiO_2 nanoparticles and the growth of TiO_2 particles in the annealing process.

4.3.3 light absorption spectrum

Fig. 4.8 shows the typical UV-visible diffuse reflectance spectrum (UV-DRS) of the annealed TiO_2 and Ag-TiO_2 nanoparticulate films with various Ag concentration. The spectrum of pure TiO_2 has an intense absorbance of UV light. The light absorption of Ag-TiO_2 nanoparticulate films is higher than that of the pure TiO_2 film in the visible light region (400–800 nm). The light absorbance of Ag-TiO_2 nanoparticulate films increased with increasing Ag concentration. The strong and broad peaks appeared around 450 nm which is due to the localized surface plasmon resonance effect of the Ag nanoparticles. It is confirmed that the addition of Ag nanoparticles into TiO_2 matrix enhances the light absorbance of TiO_2 in the visible region.

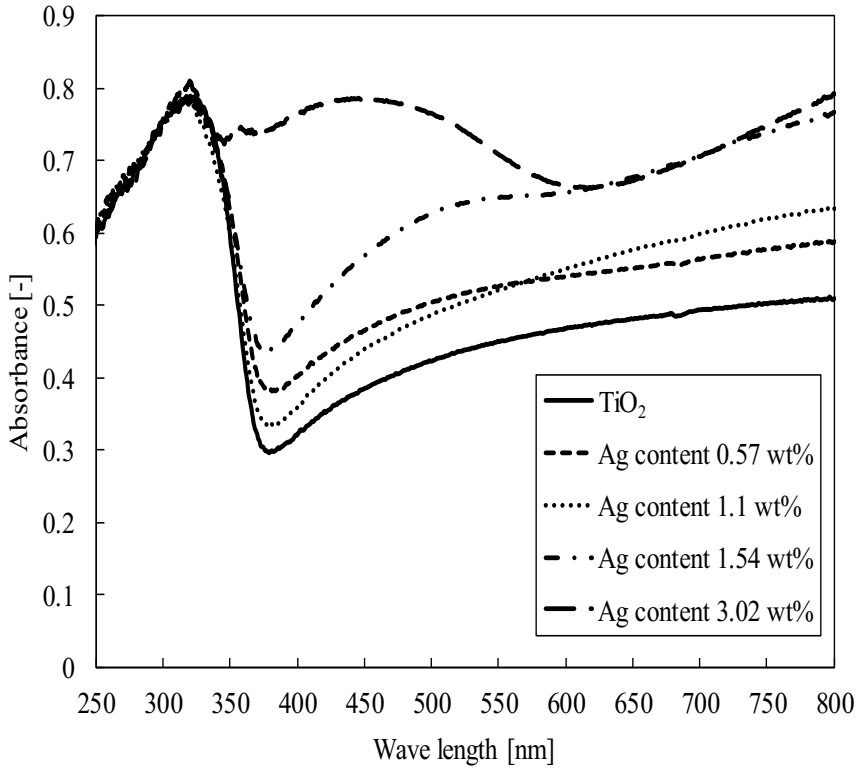

Fig. 4.8. UV-DRS of the annealed TiO_2 and Ag-TiO_2 nanoparticulate films with various Ag concentration.

4.3.4 Adsorption of dye solution of pristine TiO_2 film

The photocatalytic process of TiO_2 and Ag-TiO_2 films is constant of two steps: adsorption and the reaction. The adsorption of dye molecules on TiO_2 nanoparticles is the first step of the photocatalytic process, and the adsorption of dye molecules should be divided with the photodegradation of dye solution.

The prepared pristine TiO_2 films were put in the MB solution and R6G solution, and the intensity of dye solution was measured by UV-Vis to investigate the adsorption of dye solution. Fig. 4.9 shows the intensity of change of MB and R6G solution measured by the UV-vis every half hour without light. The intensity of R6G solution showed no

decrease after 3h standing. The influence of adsorption in R6G can be neglected. However, the intensity of MB solution showed a slow decrease. The results showed that the adsorption of R6G molecule was fast, while the adsorption of MB molecule was slow. The reason of the difference in adsorption time needs to be clarified in the future.

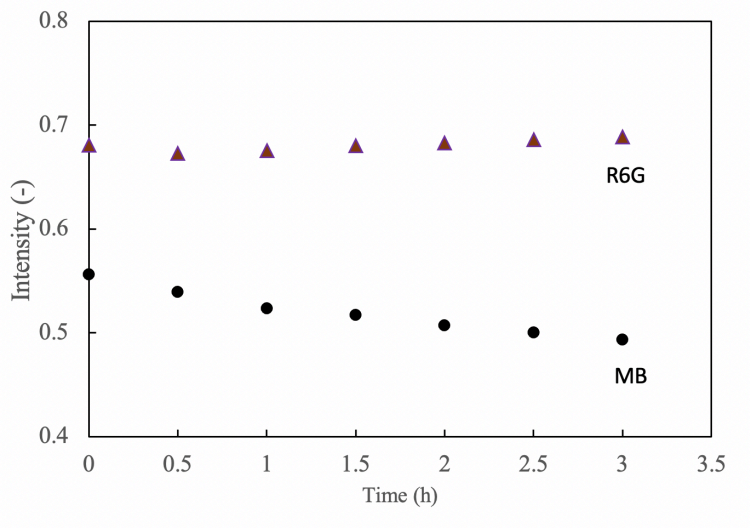

Fig. 4.9 The intensity change of MB and R6G solution measured by the UV-vis every half hour without light irradiation.

4.3.5 Photocatalytic activities of Ag-TiO_2 nanoparticulate films under UV light

To get the adsorption equilibrium, the prepared Ag-TiO_2 nanoparticulate thin films with mixture of MB solution were put in a dark chamber for 12h. Fig. 4.10 shows the photocatalytic activities of the annealed TiO_2 and Ag-TiO_2 nanoparticulate films with different Ag concentration based on the photocatalytic degradation of MB solution. The photocatalytic activity of prepared films showed an increase below 2.2 wt% and a decrease above 2.2 wt%. The optimal Ag concentration for the photocatalytic activity of

Ag-TiO_2 nanoparticulate films was obtained when the Ag concentration was 2.2 wt%. The optimal photocatalytic activity of Ag-TiO_2 nanoparticulate films was about 5.5 times than that of the annealed TiO_2 film. Moreover, the photocatalytic activity of Ag-TiO_2 nanoparticulate film was lower than that of annealed TiO_2 film.

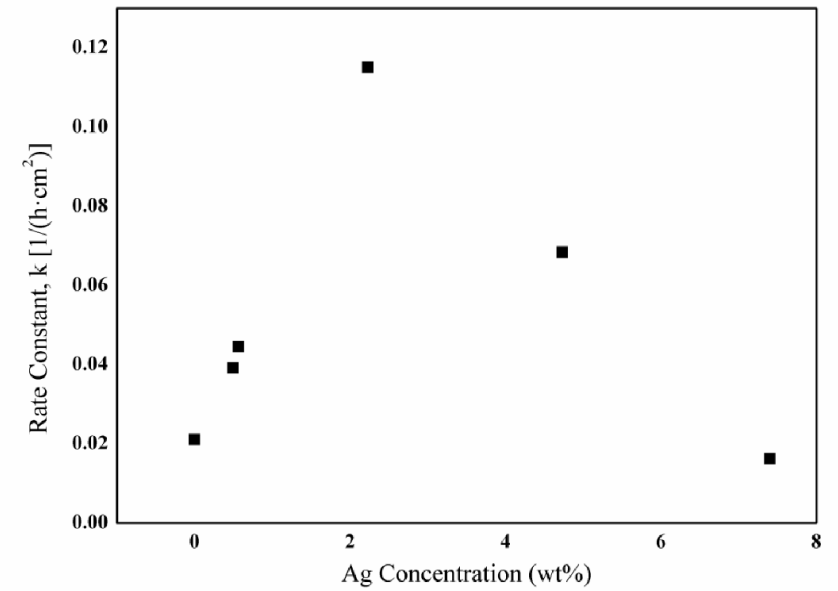

Fig. 4.10 The photocatalytic activity of annealed TiO_2 and Ag-TiO_2 nanoparticulate films with different Ag concentration based on the photocatalytic degradation of MB solution irradiated by UV light.

As we know, the photocatalytic activity is influenced by the morphological changes, crystal changes and loading concentration in the prepared Ag-TiO_2 nanocomposites (Liu *et al.*, 2004；Sung-Suh *et al.*, 2004；Tan *et al.*, 2011). The existence of Ag can reduce the recommendation of electron-hole pairs which can enhance the photocatalytic activity of TiO_2 (He *et al.*, 2002； Zhao *et al.*, 2012). The positive influence of loading Ag make the photocatalytic activity increased with increasing Ag concentration (below 2.2 wt%).

However, the photocatalytic activity of Ag-TiO_2 nanoparticulate films showed a decrease when the Ag concentration was above 2.2 wt%. The particle size of the TiO_2 nanoparticles increased heavily when the Ag concentration was above 2.2 wt% (Fig. 4.9). The increasing TiO_2 nanoparticles will decrease the specific surface area. Previous research showed that the relatively low specific surface area had a negative effect on the photocatalytic activity (Lin *et al.*, 2006). The increased particle size of TiO_2 nanoparticles was in coincidence with the significant decrease in the photocatalytic activity when the Ag concentration increased from 2.2 wt% to 7.4 wt%. Therefore, The Ag concentration in Ag-TiO_2 nanoparticulate films determined the photocatalytic activity of Ag-TiO_2 nanoparticulate films. When the Ag concentration was below 2.2 wt%, the increasing Ag concentration can inhibit the recommendation rate of electron-hole pairs in TiO_2. However, when the Ag concentration was above 2.2 wt%, the increasing Ag concentration can increase the particle size of TiO_2 in the heat treatment which dominated the decrease of photocatalytic activity of Ag-TiO_2 nanoparticulate films

Moreover, the well dispersed Ag nanoparticles on the surface of TiO_2 may block the incident UV light, which will reduce the generation of photogenerated electrons. This is another reason of decreasing photocatalytic activity when the Ag concentration was above 2.2 wt%. Hence, the photocatalytic activity of Ag-TiO_2 film with an Ag concentration of 7.4 wt% showed a worse photocatalytic performance than that of TiO_2 and other Ag-TiO_2 nanoparticulate films due to large particle size and heavy loading of Ag nanoparticles.

4.3.6 Photocatalytic activities of Ag-TiO_2 nanoparticulate films under visible light

Fig. 4.11 shows the photocatalytic activity of the annealed TiO_2 and Ag-TiO_2 nanoparticulate films estimated by measuring the degradation of rhodamine 6G solution under visible light irradiation.

The photocatalytic activity of prepared films showed an increase below 0.24 wt% and a decrease above 0.24 wt%. The optimal Ag concentration for the photocatalytic activity of Ag-TiO_2 nanoparticulate films was obtained when the Ag concentration was 0.24 wt%. The optimal photocatalytic activity of Ag-TiO_2 nanoparticulate films was about 2.4 times than that of the annealed TiO_2 film. The P25 was use as a reference. The optimal photocatalytic activity of Ag-TiO_2 nanoparticulate film showed a better photocatalytic activity than that of P25.

The positive effect of Ag nanoparticles on the photocatalytic performance of Ag-TiO_2 nanoparticulate films lead to an increase when the Ag concentration was below 0.24 wt%. Due to the LSPR effect, the Ag nanoparticles can absorb the visible light and the exited electron can transfer from Ag to TiO_2 which reduce the recommendation of electron-hole pairs. More loading Ag nanoparticles, more photogenerated electrons in the photocatalytic reaction of Ag-TiO_2 nanoparticulate films. Therefore, the photocatalytic activity of Ag-TiO_2 nanoparticulate films. films showed an increase when the Ag concentration below 0.24 wt%. But why the photocatalytic activity of Ag-TiO_2

nanoparticulate films decreased when the Ag concentration was above 0.24 wt%? The reason can be explained by two reasons.

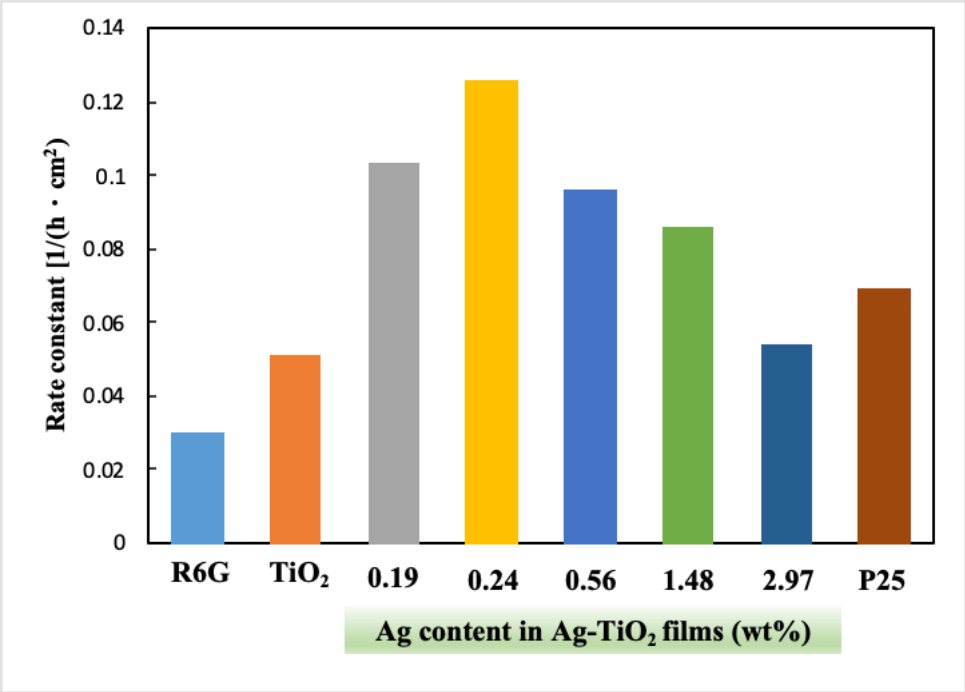

Fig. 4.11 Visible-photocatalytic activity of the pristine TiO_2 and Ag-TiO_2 nanocomposite films.

On one hand, the particle size of the TiO_2 nanoparticles increases with increasing Ag content as shown in Fig. 4.7. the surface area of TiO_2 nanoparticles will decreased in resulting of decreasing active sites in photocatalytic reaction. Therefore, the photocatalytic activity of Ag-TiO_2 nanoparticulate films showed a decrease when the Ag concentration exceed 0.24 wt%.

On the other hand, the increasing of Ag content on the surface of TiO_2 lead agglomeration of Ag nanoparticles. In the Fig. 4.3, The Ag nanoparticle size is also

changed by increasing furnace temperature. Many researchers have reported the increasing Ag particle size can influence the LSPR effect, and big Ag nanoparticles are easy to be a recombination center which will decrease the photocatalytic performance of prepared Ag-TiO_2 nanoparticulate films in high Ag concentration. Hence, the photocatalytic activity of Ag-TiO_2 nanoparticulate film start to decrease when the Ag content exceed 0.24 wt% due to the two negative effects mentioned above.

4.3.7 Difference of optimal Ag concentration under UV and visible light

The optimal Ag concentration in Ag-TiO_2 film was 2.4 wt% under UV light while the highest Ag concentration in Ag-TiO_2 film yielded at 0.24 wt% under visible light. The difference of the optimal Ag concentration is discussed as follows.

1) The mechanism of the UV-light Ag-TiO_2 photocatalyst and visible-light Ag-TiO_2 photocatalyst is different and the optimal Ag concentration under UV and visible light cannot be compared directly. Under UV light, the photoelectrons generate in the TiO_2 and transfer to the Ag, and the separated electrons and holes reacted with absorbed water and oxygen molecules. Under visible light, the photoelectrons generate in the Ag nanoparticles due to the LSPR effect and transfer to the TiO_2, and the separated electrons and holes reacted with absorbed water and oxygen molecules. Therefore, the difference in the mechanism of photocatalytic reaction under UV light and visible light leads to the difference of optimal Ag concentration.

2) The optimal Ag concentration in Ag-TiO_2 film yielded at 0.24 wt% when the Ag-TiO_2 was irradiated by visible light. Why the optimal Ag concentration was obtained in such a low amount under visible light? Usually, the particle size of Ag nanoparticle increased with Ag concentration. The Fermi level of TiO_2 is higher than that of loading Ag nanoparticles. The smaller particle size of Ag nanoparticles, the higher transfer efficiency of photoelectrons from TiO_2 to Ag. The better separation of electrons and holes can be achieved with smaller particle size of Ag nanoparticles in low Ag concentration. In other words, the photocatalytic activity is very sensitive to the size of Ag nanoparticle. The increase of Ag concentration can increase the particle size of Ag nanoparticle which result in worse photocatalytic activity. In the previous study on the effect of particle size of Ag, the optimal Ag concentration was obtained at 1–4.39 nm (Han *et al.*, 2011； Jiang *et al.*, 2014). In this study, the low Ag concentration leaded to small particle size of Ag nanoparticle, which enhanced the photocatalytic activity of Ag-TiO_2 films. The effect of Ag nanoparticle size on the photocatalytic activity of Ag-TiO_2 photocatalyst need to be classify in the future work.

4.4 Conclusions

The effect loading concentration of Ag nanoparticle on the photocatalytic performance of annealed TiO_2 and Ag-TiO_2 nanoparticulate films based on the morphological analysis, crystal analysis, elemental analysis and optical analysis. The Ag concentration in the Ag-TiO_2 nanoparticulate films can be changed by the furnace

temperature and the number density of Ag nanoparticles on the surface of TiO_2 increased with increasing Ag concentration. As the Ag concentration increased, the particle size of the Ag-TiO_2 nanoparticulate film increased especially above 2.2 wt%. It is also confirmed that the addition of Ag nanoparticles into TiO_2 matrix enhances the light absorbance of TiO_2 in the visible region, and the light absorbance ability of Ag-TiO_2 nanoparticulate films increased with increasing Ag concentration in the visible region. The photocatalytic activity of Ag-TiO_2 nanoparticulate films reached its optimum value at 2.2 wt% Ag under UV light and 0.24 wt% under visible light.

The Ag concentration is considered as a key factor for the photocatalytic activity of Ag-TiO_2 nanoparticulate films. When the Ag concentration was below 2.2 wt%, the increasing Ag concentration can inhibit the recommendation rate of electron-hole pairs in TiO_2. However, when the Ag concentration was above 2.2 wt%, the increasing Ag concentration can increase the particle size of TiO_2 in the heat treatment which dominated the decrease of photocatalytic activity of Ag-TiO_2 nanoparticulate films.

References

Chao, H. E., Y. U. Yun, H. U. Xingfang and A. Larbot, "Effect of silver doping on the phase transformation and grain growth of sol-gel titania powder" *Journal of the European Ceramic Society*, **23**, 1457-1464 (2003).

Chen, D., Q. Chen, L. Ge, L. Yin, B. Fan, H. Wang, H. Lu, H. Xu, R. Zhang and G. Shao, "Synthesis and Ag-loading-density-dependent photocatalytic activity of Ag@ TiO_2 hybrid nanocrystals" *Applied Surface Science*, **284**, 921-929 (2013).

Dehimi, M., T. Touam, A. Chelouche, F. Boudjouan, D. Djouadi, J. Solard, A. Fischer, A. Boudrioua and A. Doghmane, "Effects of Low Ag Doping on Physical and Optical Waveguide Properties of Highly Oriented Sol-Gel ZnO Thin Films" *Advances in Condensed Matter Physics*, **2015**, 1-10 (2015).

García-Serrano, J., E. Gómez-Hernández, M. Ocampo-Fernández and U. Pal, "Effect of Ag doping on the crystallization and phase transition of TiO_2 nanoparticles" *Current Applied Physics*, **9**, 1097-1105 (2009).

Gunawan, C., W. Y. Teoh, C. P. Marquis, J. Lifia and R. Amal, "Reversible antimicrobial photoswitching in nanosilver" *Small*, **5**, 341-344 (2009).

Han, R., X. Zhang, L. Wang, R. Dai and Y. Liu, "Size-dependent photochromism-based holographic storage of Ag/TiO_2 nanocomposite film" *Applied Physics Letters*, **98**, 221905 (2011).

He, C., Y. Yu, X. Hu and A. Larbot, "Influence of silver doping on the photocatalytic activity of titania films" *Applied Surface Science*, **200**, 239-247 (2002).

Hirakawa, T. and P. V. Kamat, "Charge separation and catalytic activity of Ag@ TiO_2 core− shell composite clusters under UV− irradiation" *Journal of the American Chemical Society*, **127**, 3928-3934 (2005).

Jiang, Z., Q. Ouyang, B. Peng, Y. Zhang and L. Zan, "Ag size-dependent visible-light-responsive photoactivity of Ag–TiO_2 nanostructure based on surface plasmon resonance" *Journal of Materials Chemistry A*, **2**, 19861-19866 (2014).

Kubo, M., Y. Ishihara, Y. Mantani and M. Shimada, "Evaluation of the factors that influence the fabrication of porous thin films by deposition of aerosol nanoparticles" *Chemical Engineering Journal*, **232**, 221-227 (2013).

Lin, H., C. P. Huang, W. Li, C. Ni, S. I. Shah and Y.-H. Tseng, "Size dependency of nanocrystalline TiO_2 on its optical property and photocatalytic reactivity exemplified by 2-chlorophenol" *Applied Catalysis B: Environmental*, **68**, 1-11 (2006).

Liu, S., Z. Qu, X. Han and C. Sun, "A mechanism for enhanced photocatalytic activity of silver-loaded titanium dioxide" *Catalysis Today*, **93**, 877-884 (2004).

Mosquera, A. A., J. M. Albella, V. Navarro, D. Bhattacharyya and J. L. Endrino, "Effect of silver on the phase transition and wettability of titanium oxide films" *Sci Rep*, **6**, 1-14 (2016).

Sung-Suh, H. M., J. R. Choi, H. J. Hah, S. M. Koo and Y. C. Bae, "Comparison of Ag deposition effects on the photocatalytic activity of nanoparticulate TiO_2 under visible and UV light irradiation" *Journal of Photochemistry and Photobiology A: Chemistry*, **163**, 37-44 (2004).

Suwarnkar, M. B., R. S. Dhabbe, A. N. Kadam and K. M. Garadkar, "Enhanced photocatalytic activity of Ag doped TiO_2 nanoparticles synthesized by a microwave assisted method" *Ceramics International*, **40**, 5489-5496 (2014).

Tan, T. T. Y., C. K. Yip, D. Beydoun and R. Amal, "Effects of nano-Ag particles loading on TiO_2 photocatalytic reduction of selenate ions" *Chemical Engineering Journal*, **95**, 179-186 (2003).

Tan, Y. N., C. L. Wong and A. R. Mohamed, "An Overview on the Photocatalytic Activity of Nano-Doped-TiO_2 in the Degradation of Organic Pollutants" *ISRN Materials Science*, **2011**, 1-18 (2011).

Wang, R.-C., Y.-S. Gao and S.-J. Chen, "Simple synthesis and size-dependent surface-enhanced Raman scattering of Ag nanostructures on TiO_2 by thermal decomposition of silver nitrate at low temperature" *Nanotechnology*, **20**, 375605 (2009).

Xin, B., L. Jing, Z. Ren, B. Wang and H. Fu, "Effects of simultaneously doped and deposited Ag on the photocatalytic activity and surface states of TiO_2" *The Journal of Physical Chemistry B*, **109**, 2805-2809 (2005).

You, X., F. Chen, J. Zhang and M. Anpo, "A novel deposition precipitation method for preparation of Ag-loaded titanium dioxide" *Catalysis Letters*, **102**, 247-250 (2005).

Yu, J., J. Xiong, B. Cheng and S. Liu, "Fabrication and characterization of Ag–TiO_2 multiphase nanocomposite thin films with enhanced photocatalytic activity" *Applied Catalysis B: Environmental*, **60**, 211-221 (2005).

Zhang, H., G. Wang, D. Chen, X. Lv and J. Li, "Tuning photoelectrochemical performances of Ag− TiO_2 nanocomposites via reduction/oxidation of Ag" *Chemistry of Materials*, **20**, 6543-6549 (2008).

Zhang, P., C. Shao, X. Li, M. Zhang, X. Zhang, Y. Sun and Y. Liu, "In situ assembly of well-dispersed Au nanoparticles on TiO_2/ZnO nanofibers: A three-way synergistic heterostructure with enhanced photocatalytic activity" *Journal of hazardous materials*, **237**, 331-338 (2012).

Zhang, Z., C. Shao, P. Zou, P. Zhang, M. Zhang, J. Mu, Z. Guo, X. Li, C. Wang and Y. Liu, "In situ assembly of well-dispersed gold nanoparticles on electrospun silica nanotubes for catalytic reduction of 4-nitrophenol" *Chemical Communications*, **47**, 3906-3908 (2011).

Zhao, C., A. Krall, H. Zhao, Q. Zhang and Y. Li, "Ultrasonic spray pyrolysis synthesis of Ag/TiO_2 nanocomposite photocatalysts for simultaneous H_2 production and CO_2 reduction" *International Journal of Hydrogen Energy*, **37**, 9967-9976 (2012).

Chapter 5

Summary

5.1 Conclusions

In this thesis, a gas-phase method for preparing Ag-TiO_2 nanoparticulate thin films by a combined PECVD and PVD process has been successfully developed. The morphological analysis, crystal analysis, optical analysis and resulting photocatalytic activity of prepared Ag-TiO_2 nanoparticulate thin films were investigated by changing annealing temperature and Ag contents. For the conclusions of the dissertation, the results can be described as following

The Ag-TiO_2 nanoparticulate thin films were successfully fabricated via a combined PECVD and PVD process has been successfully developed. The particle size of TiO_2 and Ag contents in prepared Ag-TiO_2 nanoparticulate thin films can be easily adjusted by changing annealing temperature and furnace temperatures respectively. This one-step gas-phase deposition process also has advantages in preparing extremely small metallic Ag nanoparticles (3–5 nm) without agglomeration, residues, complex preparation steps, and introducing Ag ions from source. This one-step gas-phase deposition process can also be used in fabricating metal-semiconductor materials which have potential in photocatalysis, gas sensor, solar cell, disinfection and hydrogen evolution aspects.

The effects of annealing temperature on the crystal structure, particle size, film thickness, and photocatalytic performance of Ag-TiO_2 nanoparticulate thin films prepared by the combined PECVD and PVD systems have been investigated. Significant difference

in particle size was observed when the prepared films were annealed with various temperatures (300–100 ºC). Not only the crystalline size but also the particle size in the Ag-TiO_2 nanoparticulate thin films increased with increasing annealing temperature while the thickness showed a decrease. Phase content in the Ag-TiO_2 nanoparticulate thin films were influenced by the various annealing temperature. As annealing temperature increased, the crystal structure experienced changes from amorphous to pure anatase to mixture of anatase and rutile to pure rutile. The best photocatalytic activity was found at the annealing temperature of 700 ℃, which includes anatase phase (77%) and rutile phase (23%). The photocatalytic activity of anatase-rutile phase is better than that of pure anatase phase, and the photocatalytic activity of pure anatase phase is better than that of pure rutile phase.

The effects of loading concentration of Ag nanoparticles on the photocatalytic activity of Ag-TiO_2 nanoparticulate films prepared by the combined PECVD and PVD systems have been investigated. Due to the presence of Ag nanoparticles on the surface of TiO_2 nanoparticles, the morphology, crystallinity and optical property of the prepared Ag-TiO_2 nanoparticulate film were heavily influenced. The loading of Ag nanoparticles in Ag-TiO_2 nanoparticulate film led to an increase in the particle size and light absorbance in visible region and a decrease of phase transition temperature when the Ag concentration increased. The photocatalytic activity of Ag-TiO_2 was strongly influenced by the Ag content through the combined effects of morphology and particle size (of TiO_2) and reached its optimum value at 2.2 wt% Ag under UV light and 0.24 wt% under visible

light. The photocatalytic activity of Ag-TiO_2 nanoparticulate films reached its optimum value at 2.2 wt% Ag under UV light and 0.24 wt% under visible light. The Ag concentration is considered as a key factor for the photocatalytic activity of Ag-TiO_2 nanoparticulate films. When the Ag concentration was below 2.2 wt%, the increasing Ag concentration can inhibit the recommendation rate of electron-hole pairs in TiO_2. However, when the Ag concentration was above 2.2 wt%, the increasing Ag concentration can increase the particle size of TiO_2 in the heat treatment which dominated the decrease of photocatalytic activity of Ag-TiO_2 nanoparticulate films.

5.2 Suggestions for Further Investigations

Based on the successful development of the one-step deposition process and the key foundlings from the evaluation of the photocatalytic Ag-TiO_2 nanoparticulate thin films fabricated by the one-step gas-phase deposition process, the suggestion for further investigations can be addressed as follows:

The one-step process not only can prepare Ag-TiO_2 nanoparticulate films but also has potential in fabricating metal-semiconductor heterogenous materials. The other noble nanoparticles such as gold, platinum and copper can also be produced similarly by vaporizing pure metal source or their mixture. Moreover, the other supporting materials such as ZnO can be prepared by changing supplied precursors.

The particle size of Ag nanoparticles is very important to the photocatalytic activity. The effect of Ag nanoparticle size on the photocatalytic activity of Ag-TiO2 photocatalyst need to be classify in the future work by using the one-step gas-phase deposition process.

The addition of Ag nanoparticle reduced the anatase-to-rutile transition temperature and increased the particle size of TiO_2 in the heat treatment. The mechanism of the change in crystal structure, particle size and their relationship need to be derived.

In evaluation of the photocatalytic activity of Ag-TiO_2 nanoparticulate thin films, the addition of Ag nanoparticles on the surface of TiO_2 nanoparticles exhibits positive effects of inhibiting electron-hole recombination and reducing anatase-to-rutile transformation temperature. However, the particle size of TiO_2 nanoparticles in Ag-TiO_2 nanoparticulate thin films increased with increasing Ag concentration which is considered as a negative factor for photocatalytic activity. The design in preparations of new Ag-TiO_2 photocatalytic nanocomposites should consider the opposite effects.

Appendix I: List of Figures

Appendix II: List of Tables

Appendix III: List of Publications

This dissertation was partly written based on the following publications written in the period of doctoral course.

1. K. Kusdianto, **Dianping Jiang**, Masaru Kubo, and Manabu Shimada, "Fabrication of TiO_2–Ag nanocomposite thin films via one-step gas-phase deposition", *Ceramics International*, **43**(6): 5351-5355 (2017)
2. K. Kusdianto, **Dianping Jiang**, Masaru Kubo, and Manabu Shimada, "Effect of annealing temperature on the photocatalytic activity of Ag–TiO_2 nanocomposite films by one-step gas-phase deposition", *Materials Research Bulletin*, 97 497-505 (2018)
3. **Dianping Jiang**, K. Kusdianto, Masaru Kubo, and Manabu Shimada, "Effect of Ag loading content on morphology and photocatalytic activity of Ag-TiO_2 nanoparticulate films prepared via simultaneous plasma-enhanced chemical and physical vapor deposition", *Materials Research Express*, **7**(11): 116406 (2020)

Presentation in Conferences

1) “Preparation of photocatalytic TiO_2–Ag nanocomposite thin films by one-step gas-phase deposition”, **Dianping Jiang**, K. Kusdianto, Masaru Kubo, Manabu Shimada, International Workshop on Nanodevice Technologies 2017 (IWNT2017), P-19, 2017.3.

2) Enhanced photocatalytic activity of TiO_2–Ag nanocomposite films prepared via one-step gas-phase deposition by heat treatment”, **Dianping Jiang**, K. Kusdianto, Masaru Kubo, Manabu Shimada, Asian Aerosol Conference 2017 (AAC 2017), PS0165 PS-NM17, 2017,7.

3) Preparation and Evaluation of Photocatalytic Ag-TiO_2 Nanoparticulate Films, **Dianping Jiang**, K. Kusdianto, Masaru Kubo, Manabu Shimada, International Workshop on Nanodevice Technologies 2018 (IWNT2018), P-10, 2018.3.

4) Effect of Loading Concentration on the Photocatalytic Activity of Ag-TiO_2 Nanocomposite Films Fabricated by One-Step Gas-Phase Deposition, **Dianping Jiang**, K. Kusdianto, Masaru Kubo, Manabu Shimada, International Aerosol Conference 2018 (IAC 2018), 4MS.9, 2018.9.

5) Visible-Light Photoactivity of Photocatalytic Ag–TiO_2 Nanocomposite Thin Film Prepared via Combined Gas-phase Deposition of Nanoparticles, **Dianping Jiang,** K. Kusdianto, Masaru Kubo, Manabu Shimada, Asian Aerosol Conference 2019 (AAC 2019), Parallel Oral Session VII, 2019.5.

6) 「エアロゾル粒子の堆積による Ag/TiO_2 光触媒薄膜の作製と熱処理の影響評価」, **Dianping Jiang**, K. Kusdianto, Masaru Kubo, Manabu Shimada, 第 34 回エアロゾル科学・技術研究討論会, F-04, 2018.3.

7) 「気相堆積複合膜の構造・組成制御による光触媒の作製と評価」, **姜殿平**, 正木 佑弥, K. Kusdianto, 久保 優, 島田 学, 第 36 回エアロゾル科学・技術研究討論会, YP04, 2019.9.